14

Chemical Transformations in Inhibited Flames over Range of Stoichiometry

O.P. Korobeinichev, A.G. Shmakov and V.M. Shvartsberg
Institute of Chemical Kinetics & Combustion,
Siberian Brunch of Russian Academy of Sciences, Novosibirsk,
Russia

1. Introduction

Addition of chemically active compounds to flame, which are able to change the flame velocity, the flame propagation limits and the other macrokinetic parameters, seems to be the most effective way to control combustion. Of special interest are chemically active inhibitors producing a noticeable effect on flame at low concentrations, which do not change the flame stoichiometry. Thousands of elementary reactions involving hundreds of species proceed in hydrocarbon flame. However, the key reactions are those involving atoms and free radicals; with their reaction rates being much faster than those of the other reactions. The inhibitors mainly interact and affect the above processes.

2. Methods and approaches

2.1 Flame structure

Knowledge of the chemistry and mechanism of combustion at the molecular level makes it possible to create combustion models capable of predicting many combustion characteristics important for practice, such as the rate and completeness of combustion, temperature and composition of the products under various conditions, and also to control the process of combustion by means of selecting conditions that would ensure the required characteristics of combustion. The flame structure is the main source of information on the chemistry of combustion. One of the most effective method for studying the flame structure is probe mass spectrometry, a versatile method capable of (1) identifying the components present in the flame, (2) determining their quantitative composition (concentrations), and (3) measuring these concentrations in the combustion zone (examine the structure of these flames). An efficient approach to studying combustion chemistry is to combine experimental methods with numerical simulations within the framework of a detailed kinetic mechanism. This combination makes it possible not only to understand the chemical mechanism of the process, but also to develop a kinetic model and constantly refine it by comparing its predictions with experimental data. At present, this approach is widely used in combustion research, including its application to studying the chemistry of combustion of organophosphorus compounds (OPCs). The most efficient method for determining the chemical structure of flames is the probing molecular-beam mass spectrometry (MBMS)

with soft ionization, a technique that makes it possible to detect atoms, radicals, and labile components in the flame. It was successfully applied to studying the combustion of OPCs at the Cornel University (USA) (Werner & Cool, 1999) and at the Institute of Chemical Kinetics and Combustion of the Siberian Division of the Russian Academy of Sciences (Korobeinichev et al., 1996).

2.1.1 Molecular beam mass spectrometry

The best way to analyze the combustion products in situ is to use molecular beam sampling from the flame with the help of a sonic probe that forms a supersonic outflow of products into vacuum, which, passing through a skimmer, transforms into a molecular beam. The expansion of the products quenches chemical reactions in the sampled gases. The skimmer cuts out the central part of the flow, free from the products of possible heterogeneous catalytic reactions on the internal walls of the probe. The composition of the molecular beam is analyzed by a soft-ionization mass spectrometry. The molecular beam method ensures the preservation of the sample during extraction and transport to the analyzer. Mass spectrometry makes it possible to simultaneously detect *in situ* all flame components, a capability that is beyond the reach of any other method. Figure 1 shows the setup with molecular beam mass spectrometric sampling; for details, see (Korobeinichev et al., 1996).

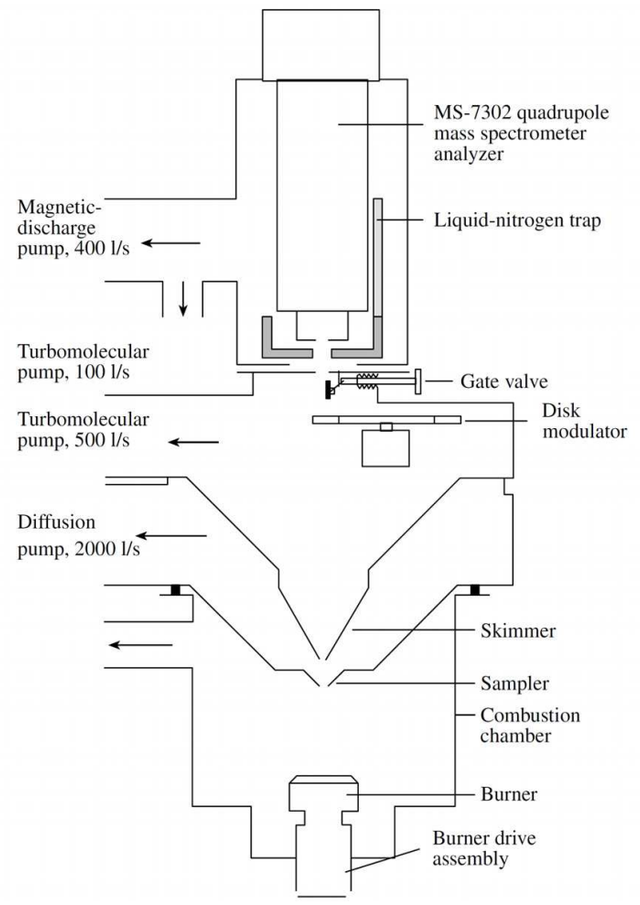

Fig. 1. Schematic of the MBMS setup for sampling gaseous flames.

The setup at the Institute of Chemical Kinetics and Combustion employed soft electron-impact ionization (7–20 eV). The low scatter of electron energies was achieved by using cathode voltage-drop compensation (Dodonov et al., 1990). This technique makes it possible to decrease the fragmentation of ions, an effect that interferes with measurements of the concentrations of atoms, radicals, and other labile species. The ionization potentials of PO, PO_2, HOPO, $HOPO_2$, and $(HO)_3PO$ were determined by measuring the ionization efficiency curves during direct sampling of flames seeded with OPCs. The accuracy of measuring the ionization potentials is determined by the ionizing electron energy scatter, signal-to-noise ratio, and intensity of the signal itself.

2.1.2 Microthermocouple measurements of the flame temperature

The temperature profiles in flames are usually measured with Pt/Pt+10% Rh thermocouples 0.05-0.02 mm in diameter. The ends of the thermocouple are welded to a 0.2-mm-diameter wire fabricated from the same material. Springs provide a steady stretching of the thermocouple and made it possible to prevent it from being deformed in the flame (Korobeinichev et al., 1996). Upon welding the surface of the thermocouple is coated with SiO_2 or Ceramobond 569 (Burton et al., 1992) to eliminate catalytic processes on its surface. The corrections for thermal emission are estimated using the formula from (Kaskan, 1957). To take into account the thermal disturbances introduced into the flame by the probe, the spatial variation of the temperature is measured with a thermocouple positioned at a distance of 0.25–0.30 mm from the probe tip.

2.2 Methods for measuring the laminar flame speed

The laminar flame speed was measured on a Mache – Hebra burner (a modification of the Bunsen burner). A quartz tube with a converging nozzle at the end appears as the burner. Such a nozzle is needed to make the visible flame contour take the shape of a regular cone. The laminar flame speed was calculated from the measured flow rate of the combustible mixture and the surface area of the flame cone. The size of the flame cone was identified with its luminescent contour or by shadow photography method. The error in determination of the flame speed by this method is 5% (for stoichiometric methane – air flame). The laminar flame speed was also measured by using the heat flux method (De Goey et al., 1993; Van Maaren et al., 1994), which makes it possible to determine this parameter with a high accuracy (±1% for a stoichiometric methane – air flame) over a wide range of compositions of the combustible mixture. The flat burner was a copper disk with small orifices; thermocouples were welded into orifices at various distances from the burner axis. The temperature of the disk was 60°C, whereas the combustible mixture temperature was 35°C. While passing through the orifices, the mixture was heated. By varying the flow rate of the combustible mixture, it is possible to achieve a uniform radial distribution of temperature over the disk surface, a situation that corresponds to the equality of the heat flux from the flame to the burner surface. In this case, the conditions of combustion are close to adiabatic. This means that the velocity of the combustible mixture equals the laminar flame speed.

2.3 Simulation of the structure and speed of a laminar flame

The simulation of the flame structure was performed using the PREMIX and CHEMKIN-II computer codes (Kee et al., 1989a 1989b), which make it possible to calculate the concentration profiles of species in a flame stabilized over a flat burner and the laminar flame speed by using a detailed mechanism composed of elementary chemical reactions and databases of thermodynamic and transport properties. Due to the existence of the heat fluxes from the flame to the sampler and burner, notably at atmospheric pressure, the flame structure was calculated employing the experimentally measured temperature profile. For this purpose, as in (Biordi et al., 1974), we used the data obtained with the help of a thermocouple located near the inlet orifice of the probe. The simplest mechanism of methane oxidation included 58 reactions and 20 species. Of these reactions, 23 belong to the hydrogen oxidation mechanism. This set of reactions was successfully used in modelling the structure of a stoichiometric hydrogen – oxygen flame stabilized over a flat burner at a pressure of 47 Torr (Korobeinichev et al., 1999a, 1999b, 2000) and of lean methane – oxygen flame stabilized at 76 Torr (Korobeinichev et al., 1999c, 2001). The structure and laminar flame speed of methane – oxygen flames at atmospheric pressure was calculated using the GRI 3.0 mechanism (Smith et al., 1999), a more complex kinetic mechanism composed of 325 reactions involving 53 species. The structure of propane – oxygen flames was simulated using 469 reactions involving 77 species (Curran et al., 2003, 2004). The structure of hydrogen – oxygen flames seeded with trimethylphosphate (TMP) and Dimethylmethylphosphonate (DMMP) was determined using a kinetic model of OPCs destruction in flames involved 35 steps. This model was initially developed on the basis of experimental data on the structure of flames seeded with DMMP (Werner & Cool, 1999; Korobeinichev et al., 1996), thermochemical data obtained by Melius, and the mechanism proposed by Twarowski (Twarowski, 1993a, 1993b, 1995); it was tested by comparing the experimental and theoretical results on the structure of H_2 – O_2 – Ar flames seeded with TMP and DMMP (Korobeinichev et al., 1999b, 2000, 2001) at a pressure of 47 Torr and methane – oxygen flames seeded with TMP at 76 Torr (Korobeinichev et al., 2001). This model includes the mechanism developed by Twarowski (Twarowski, 1993a, 1993b, 1995) with modified rate constants from (Korobeinichev et al., 2000). Later, the model was refined by altering the rate constants of six key steps and was successfully applied to calculating the structure of flames at atmospheric pressure. The enthalpies of formation of phosphorus oxyacids were calculated by various quantum-chemical methods (Glaude et al., 2000; Mackie et al., 2002; Korobeinichev et al., 2005). At the same time, the enthalpies of formation of some activated complexes were calculated by varying their structures (intermediate states) for different pathways of the key reactions. As a result, it was found that some of the steps in the mechanism of the destruction of OPCs are nonelementary, consisting of a sequence of elementary transformations (Korobeinichev et al., 2005, Jayaweera et al., 2005). Based on the calculations performed, the authors of (Korobeinichev et al., 2005, Jayaweera et al., 2005) developed a more detailed mechanism of the destruction of OPCs, which, in addition, was capable of describing propane – air mixtures of various compositions at atmospheric pressure. This mechanism consists of 210 reactions and 41 phosphorus-containing species.

3. Phosphorus containing compounds

3.1 Inhibition and promotion. Low-pressure hydrogen flames

One of the most interesting finding, made during investigation of OPCs combustion chemistry, is the promotion effect of phosphorus-containing compounds on hydrogen low-pressure flames.

Hastie and Bonnell (Hastie & Bonnell, 1980) studied the effect of TMP on atmospheric-pressure methane–oxygen and hydrogen–oxygen flames of various types and compositions by using MBMS and optical and spectroscopic methods. Although these authors have not observed flame promotion but inhibition only, they proposed reactions for flame inhibition via H and OH recombination catalyzed by phosphorus-containing compounds. Analyzing the proposed mechanism Hastie and Bonnell suggested that this kinetic scheme can provide promotion effect.

The first experimental observations of a decrease of the flame zone and a rise of the temperature of low-pressure $H_2/O_2/Ar$ flame as TMP was added were made by Korobeinichev et al. (Korobeinichev et al., 1994, 1996) (see Fig. 2). This phenomenon was termed promotion. The singularity of the phenomenon consisted in the following. A decrease in the width of the flame zone and a rise in the flame temperature occurred simultaneously with a decrease of radicals concentration in the flame (Korobeinichev et al., 1999b, 2001). Later it was shown that the promotion effectiveness for a stoichiometric flame at 47 Torr increases with OPCs loading and riches its maximum at concentration of 0.6% by volume (Korobeinichev et al., 2001). A further increase of OPCs loading results in a drop of the flame speed (Fig. 3).

It is noteworthy that Korobeinichev and co-authors (Korobeinichev et al., 1999d) measured concentration profiles of phosphorus oxides and acids PO, PO_2, HOPO, $HOPO_2$, and $(HO)_3PO$ in the flame that are the key flame species responsible for H and OH catalytic recombination. In the same work the authors demonstrated that the same chemical processes are responsible for both promotion and inhibition.

Twarowski (Twarowski, 1993a 1993b, 1995) made a significant progress in understanding the chemistry of catalytic recombination of H and OH with participation of phosphorus-containing flame species. Using a flash photolysis method, Twarowski studied the rate of H and OH recombination in the sampled combustion products (T=2000 K) of $H_2/O_2/Ar/P_2H_6$ flame. A phosphine additive was demonstrated to accelerate H and OH recombination. Twarowski assumed this process to be a recombination of H and OH radicals catalyzed by phosphorus oxides and acids (PO, PO_2, HOPO, and $HOPO_2$). He developed a reaction mechanism for phosphorus-catalyzed recombination. Later Twarowski refined his model (Twarowski, 1996).

A more detailed explanation of the nature of the promotion effect was given by Bolshova and Korobeinichev (Bolshova & Korobeinichev, 2006). The authors simulated the structure and speed of various low-pressure and atmospheric-pressure flames with various equivalence ratios. The authors revealed the influence of equivalence ratio on the inhibition and promotion effectiveness. In particular, the lean $H_2/O_2/Ar$ flames were shown to be promoted most effectively and the promotion efficiency decreased as the equivalence ratio

rose. As to inhibition, an inverse dependence was observed: higher inhibition efficiency was observed for richer atmospheric-pressure $H_2/O_2/Ar$ flames.

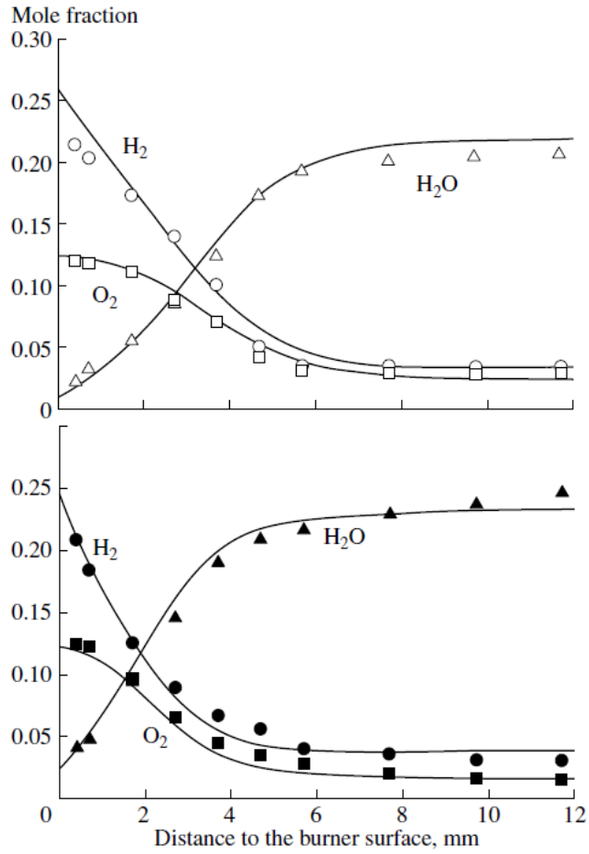

Fig. 2. Effect of a 0.2% TMP additive (lower plot) on the concentration profiles of the stable components of a hydrogen–oxygen flame stabilized over a flat burner at a pressure of 47 Torr; the points and lines are the experimental and simulation results, respectively.

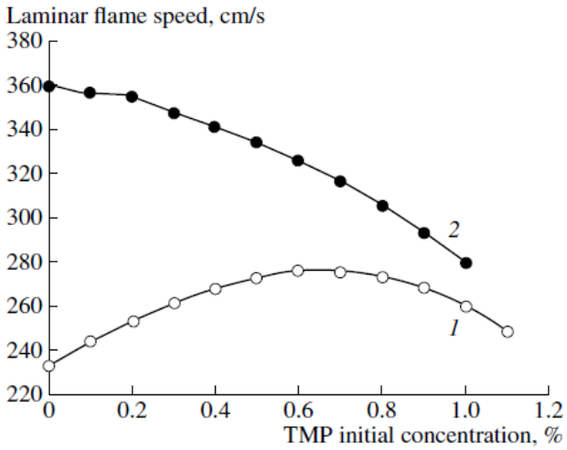

Fig. 3. Dependence of the speed of hydrogen–oxygen–TMP flame on the initial concentration of TMP at (*1*) 47 and (*2*) 760 Torr.

Bolshova and Korobeinichev performed the sensitivity analysis and revealed that a rise of low-pressure $H_2/O_2/Ar$ flame speed, as TMP loading is increased, is accompanied by a rise of the net rate of the chain-branching reaction $H + O_2 = O + OH$. It occurs due to a rise of the flame temperature throughout the flame zone. The flame temperature rise is explained by a release of additional heat due to catalytic pathway for water formation from H and OH. Increasing the additive loading increases both the branching rate and the chain termination rate. However, because of the high concentration of the chain carriers in low-pressure $H_2/O_2/Ar$ flames, the increase in the branching reaction rate dominates over the chain termination, resulting in the growth of the flame speed. In the case of atmospheric-pressure flames, where the radicals concentration is much lower and the catalytic recombination does not result in the flame temperature rise, the OPC addition to flame leads to a decrease in the flame speed.

It is noteworthy that OPCs additive increases the chain-termination rate, thus accelerating approach of the system to thermodynamic equilibrium. Therefore, at certain concentration, e.g. 0.6% by volume for the stoichiometric flame at 47 Torr, the promotion efficiency reaches its maximum.

3.2 Mechanism for inhibition of hydrogen flames at atmospheric pressure

3.2.1 Effect of the equivalence ratio and the degree of dilution with an inert on the speed of a $H_2/O_2/N_2$ flame doped with TMP

At present time a number of kinetic models for flame inhibition and promotion by OPCs are available. The last and the most justified version of the mechanism, which was developed on the basis of experimental results on speed of TMP-doped C_3H_8/air flames and quantum-mechanical calculations (Korobeinichev et al., 2005; Jayaweera et al., 2005) was used for predicting many experimental data including flame suppression (Shmakov et al., 2006), chemical structure of diffusive counterflow (Knyazkov et al., 2007) and premixed (Korobeinichev et al., 2007) hydrocarbon/air flames doped with OPCs. In spite of a satisfactory prediction of speed and structure of lean and stoichiometric flames, the mechanism predicted concentration profiles of labile species in rich flames with lower accuracy (Korobeinichev et al., 2007). To explain a sharp decrease of the inhibition effectiveness of hydrocarbon flames at equivalence ratio >1.2–1.3 and a disagreement between modeling and experiment (Korobeinichev et al., 2007), a formation of inactive P- and C-containing species in rich flames, which are not considered by the model was proposed. Therefore, it was important to check on this suggestion and to validate the mechanism by comparing the measured and simulated speed and structure of atmospheric-pressure $H_2/O_2/N_2$ flames of various fuel/oxidizer ratios.

Figure 4 presents the measured speeds of $H_2/O_2/N_2$ flames versus ϕ (equivalence ratio $\phi=([H_2]/[O_2])/([H_2]_{st}/[O_2]_{st})$, where $[H_2]$, $[O_2]$, $[H_2]_{st}$, $[O_2]_{st}$ – concentration of hydrogen and oxygen in studied and stoichiometric combustible mixture, respectively) in the range from 0.32 to 2.8 with the dilution ratio D ($D=[O_2]/([O_2]+[N_2])$, where $[O_2]$ and $[N_2]$ concentration of oxygen and nitrogen in combustible mixture) in the range from 0.209 to 0.077. The same figure shows data (Egolfopoulos, 1990) obtained using a counterflow burner for a combustible mixture at room temperature and converted to the conditions of our experiments ($t_0=35^0C$). Good agreement between our and literature data indicates the correctness of our measurements. The flame speeds predicted by the model are slightly lower than the experimental data.

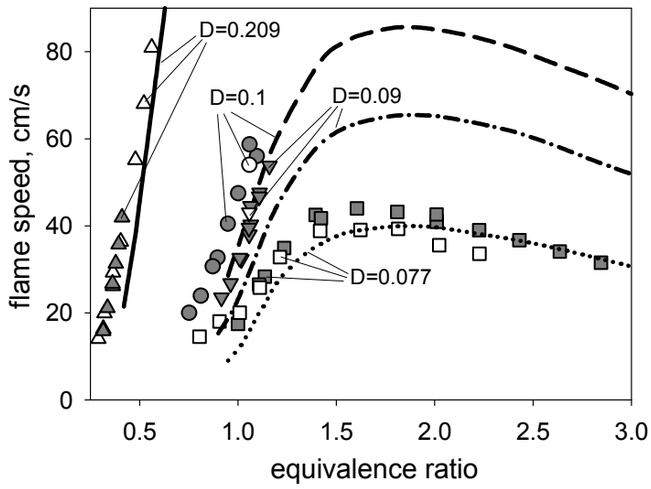

Fig. 4. Speed of $H_2/O_2/N_2$ flames with different dilution ratios (D) versus equivalence ratio; symbols – experiment (gray symbols – (Korobeinichev et al., 2009), open symbols - (Egolfopoulos & Law,1990)), lines – modeling.

The addition of 0.04% TMP (by volume) to the flames leads to a significant decrease in their speed. Figure 5 gives the measured flame speeds (symbols) and those calculated (dashed curves) using the model of (Jayaweera, 2005) versus ϕ for a flame doped with TMP. It is evident from Fig. 5 that the experimental and calculated results differ by a factor of 1.3 to 2. This difference, however, is not due to systematic measurement errors. The observed disagreements between the measured and calculated speeds are different for flames with and without TMP additives: for undoped flames, the flame speed predicted by the model is slightly underestimated, and for flames with the additive, it is overestimated.

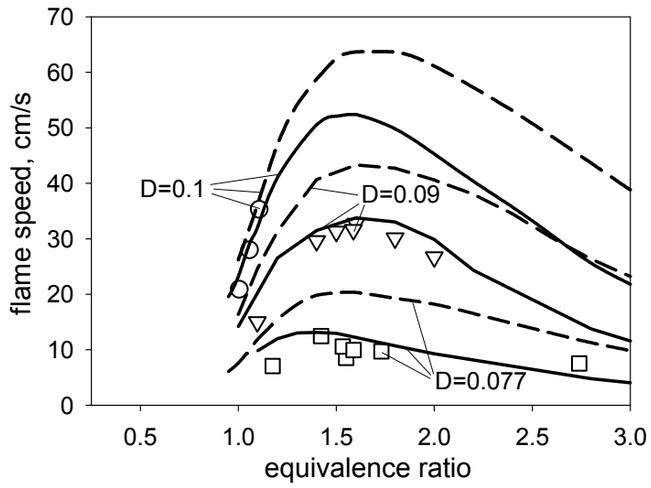

Fig. 5. Speed of $H_2/O_2/N_2$ flames doped with 0.04% TMP with different D versus equivalence ratio; symbols – experiment, dashed lines – modeling using mechanism (Jayaweera et al., 2005), solid lines – modeling using the updated mechanism.

An analysis of the speed sensitivity of a $H_2/O_2/N_2$ flame doped with TMP with respect to the rate constants of the reactions involving P-containing species shows that, in contrast to

hydrocarbon–air flames, the $H_2/O_2/N_2$ flame speed is the most significantly sensitive to the primary stages involving TMP and its primary destruction products, which proceed in the low-temperature flame zone. These reactions are given in Table 1. It should be noted that in methane–air and propane–air flames, the flame speed was most significantly affected by the atom and radical recombination reactions involving phosphorus oxyacids, which proceed in the high-temperature flame zone (Korobeinichev et al., 1999b). Because the rate constants of the stages presented in Table 1 have previously been estimated only approximately (Glaude et al., 2000), we changed the pre-exponential factors of their rate constants as is shown in Table 1 in order to obtain agreement between the calculated and measured speeds of TMP-doped flames.

Reaction	A [a], (Jayaweera et al., 2005)	$A_{modified}$[a]
$(CH_3O)_3PO + H = (CH_3O)_2PO(OCH_2) + H_2$	2.2×10^9	4.4×10^9
$(CH_3O)_2PO(OCH_2) + O = OP(OCH_3)_2O + CH_2O$	5.0×10^{13}	1.0×10^{13}
$(CH_3O)_2PO(OCH_2) = OP(OCH_3)_2 + CH_2O$	2.0×10^{13}	2.0×10^{12}

[a]Units are cm^3, mole, s.

Table 1. Three important reactions and pre-exponential factors of their rate constants before and after modification.

The results of flame speed calculations using the changed reaction rate constants are given in Fig. 5. It is evident that the changed mechanism provides an adequate description of the experimental data on the effect of TMP additives on the $H_2/O_2/N_2$ flame speed. We note that the sensitivity coefficients for the same reactions in CH_4/air flames doped with TMP are negligibly small. For example, for a CH_4/air flame (ϕ=1.1, 0.06% TMP), the flame speeds calculated for the original mechanism and the mechanism with the changed rate constants of the three reactions given above differ by only 0.2 %. Thus, the changed mechanism describes the propagation speed of both hydrocarbon–oxygen and hydrogen–oxygen flames doped with TMP. The calculations showed that the change in the rate constants of the reactions did not lead to appreciable changes in the flame structure for ϕ=1.6, including the concentration profiles of the final products of TMP conversion – PO, PO_2, HOPO and $HOPO_2$.

The changed rate constants of the three reaction were used to calculate the dependence of the inhibition effectiveness F ($F=(U_0-U)/U_0$, where U_0 and U are the speeds of the undoped flames and flames doped with 0.04 % TMP, respectively) on ϕ. The calculated dependences are presented in Fig. 6. It can be seen that F increases as ϕ increases from 1 to 3 and as D decreases from 0.209 to 0.077. Modeling data with updated mechanism for D=0.077 are in a good agreement with experiment.

It is important to note that the dependence of F on ϕ for $H_2/O_2/N_2$ differs from that for hydrocarbon flames (Korobeinichev et al., 2007; Rybitskaya et al., 2007). In hydrocarbon flames doped with 0.06% TMP, the inhibition effectiveness F increases slightly as ϕ increases from 0.7 to 1.2–1.3, and a further increase in ϕ from 1.3 to 1.5 leads to an abrupt decrease in F by a factor of 1.5 to 2 (Korobeinichev et al., 2007).

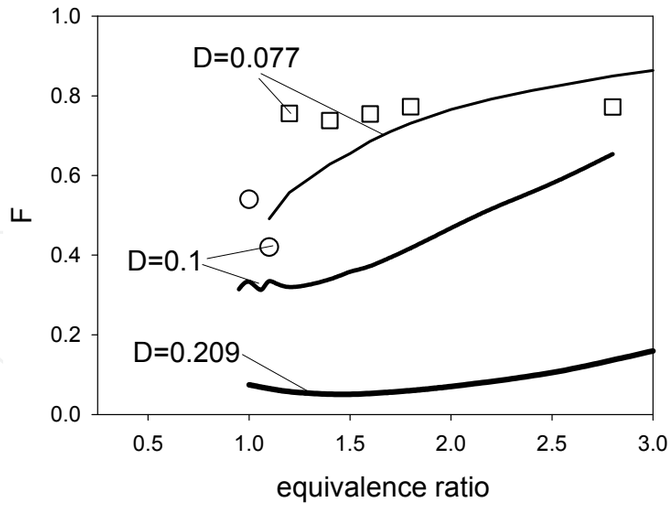

Fig. 6. Inhibition effectiveness F for $H_2/O_2/N_2$ flames doped with 0.04% TMP with different dilution ratios (D) versus equivalence ratio; symbols – experiment, lines – modeling using the updated mechanism.

The addition of TMP to flames reduces the maximum concentration of H atoms in the chemical reaction zone of a flame. Figure 7 shows the relative reduction in the maximum concentration of H atoms $\Delta[H]_{max}$ ($\Delta[H]_{max}=1-[H]^{d}_{max}/[H]^{0}_{max}$) and OH radicals $\Delta[OH]_{max}$ ($\Delta[OH]_{max}=1-[OH]^{d}_{max}/[OH]^{0}_{max}$) due to the addition of TMP versus ϕ, obtained from structure simulations for freely-propagating flames without additives and with 0.04% TMP added. Where $[H]_{max}$ and $[OH]_{max}$ – maximal concentrations of H and OH in the flame zone, subscripts "d" and "0" are related to doped and clear flames respectively. It is evident from Figs. 6 and 7, that there is a correlation between the dependences of F and $\Delta[H]_{max}$ and $\Delta[OH]_{max}$ on ϕ and D.

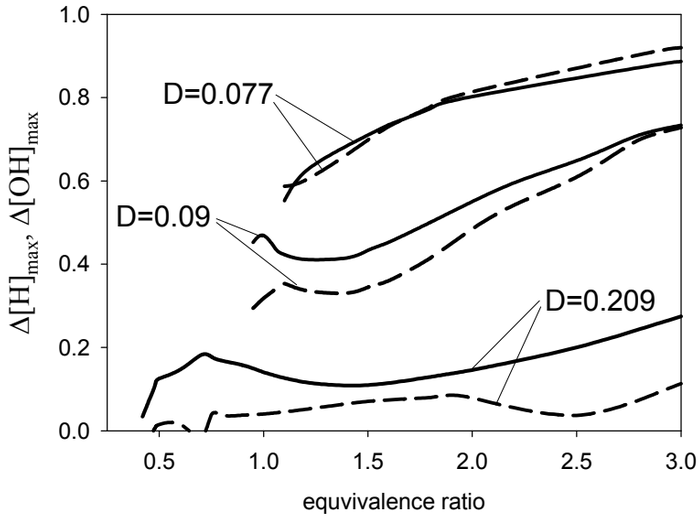

Fig. 7. Relative decrease of H (solid lines) and OH (dashed lines) maximal concentration in flames doped with 0.04% TMP with different D versus equivalence ratio; modeling data using the updated mechanism.

An analysis of the flame speed sensitivity coefficients with respect to the reaction rate constants for a flame with D=0.09 shows (Fig. 8) that an increase in ϕ from 1.1 to 1.9 primarily enhances the role of the reactions of hydrogen atoms with TMP and its primary destruction product:

$$(CH_3O)_3PO + H = (CH_3O)_2PO(OCH_2) + H_2 \quad (1)$$

$$(CH_3O)_2PO(OCH_2) + H = (CH_3O)_3PO \quad (2)$$

and the reactions with the HOPO species:

$$HOPO + H = H_2 + PO_2 \quad (3)$$

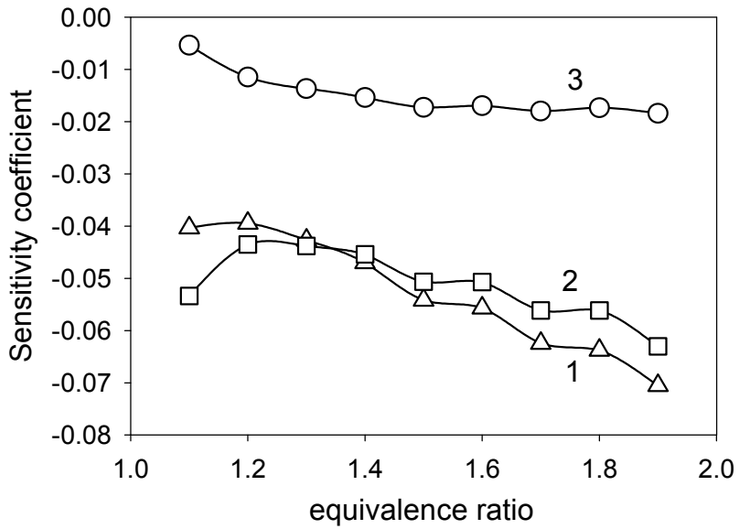

Fig. 8. Sensitivity coefficients of speed of $H_2/O_2/N_2$ flames (ϕ = 1.6, D = 0.077, 0.09, and 0.209) doped with 0.04% TMP to rate constants of reactions (1)–(3) involving P-containing species; modeling is based on mechanism (Jayaweera et al., 2005)

These reactions are involved in the catalytic recombination cycles of H atoms with the formation of H_2. It is these reactions that are responsible for the rise in the inhibition effectiveness with increasing of ϕ. Under the catalytic recombination responsible for scavenging of radicals in OPC-doped flames, all the authors meant reactions involving phosphorus oxides and acids (PO, PO_2, HOPO, and $HOPO_2$). It was assumed that organophosphorus combustion intermediates play a negligible role in the inhibition processes. However, in these specific flames reactions of OPCs with active species are of importance.

An analysis of the speed sensitivity coefficients of TMP-doped $H_2/O_2/N_2$ flames with respect to the rate constants of the main hydrogen combustion reactions and the reactions involving P-containing species revealed the main stages responsible for an increase in F with decreasing D. From the data given in Fig. 9 for the main hydrogen combustion reactions, it is evident that a decrease in D leads primarily to a growth in the role of the $H+O_2=O+OH$ branching reaction. In flames with ϕ=1.6, the flame speed sensitivity coefficient with respect

to the rate constant of this reaction increased by a factor of 4 as D decreased from 0.209 to 0.077. In addition, the sensitivity coefficient for this reaction is much larger than that of the remaining reactions. Furthermore, dilution with N_2 changes the role of the $H+O_2(+M)=HO_2(+M)$ recombination reaction, for which the sensitivity coefficient is negative for flames with dilution coefficients D=0.077 and D=0.09 and is positive for D=0.209.

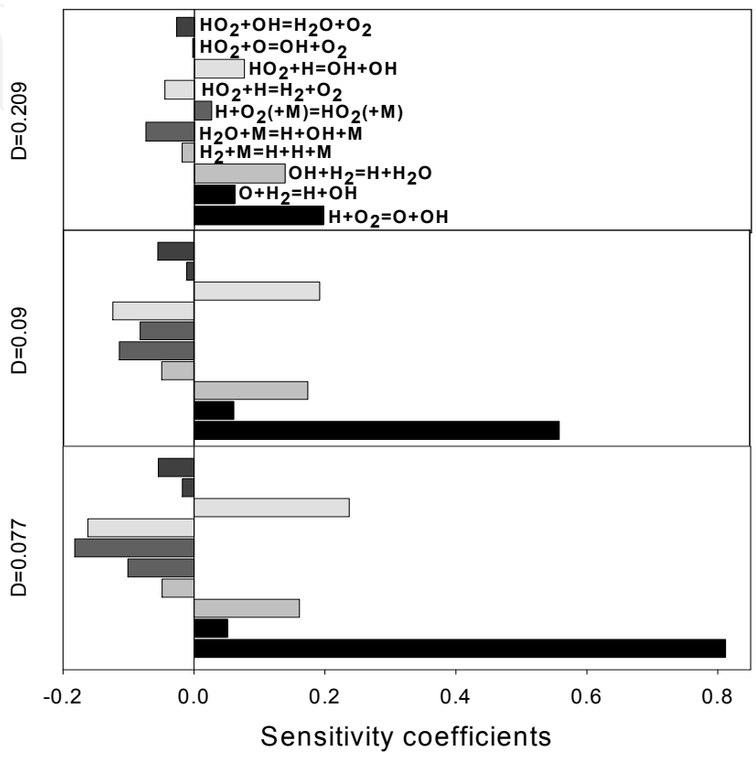

Fig. 9. Sensitivity coefficients of speed of $H_2/O_2/N_2$ flame (φ = 1.6, D = 0.077, 0.09, 0.209) doped with 0.04% TMP to rate constants of 10 key reactions of hydrogen combustion.

However, an analysis of the flame speed sensitivity to the rate constants of chain termination reactions – radical recombination upon interaction with TMP and its destruction products (Fig. 10) – shows that decreasing D increases the sensitivity to these reactions much more strongly than the sensitivity to the branching reaction constant rate. For example, as D decreases from 0.209 to 0.077, the sensitivity coefficient with respect to the rate constants of reactions (1) and (2) increases by a factor of 8 and 20 times, respectively. This is much greater than the increase in the flame speed sensitivity coefficient with respect to the branching reaction. An analysis of the simulation results shows that, a decrease in D from 0.209 to 0.077 also results in a factor of 2-5 increase in the ratio of the maximum rate of recombination of H atoms by reactions (1) and (2) to the maximum rate of the branching reaction. It is this factor that is responsible for the increase in the inhibition effectiveness F with decreasing D, and, possibly, for the increase in F with increasing of ϕ. Thus, the ratio of the chain termination rate to the chain branching rate is an important parameter that determines the hydrogen–oxygen flame speed.

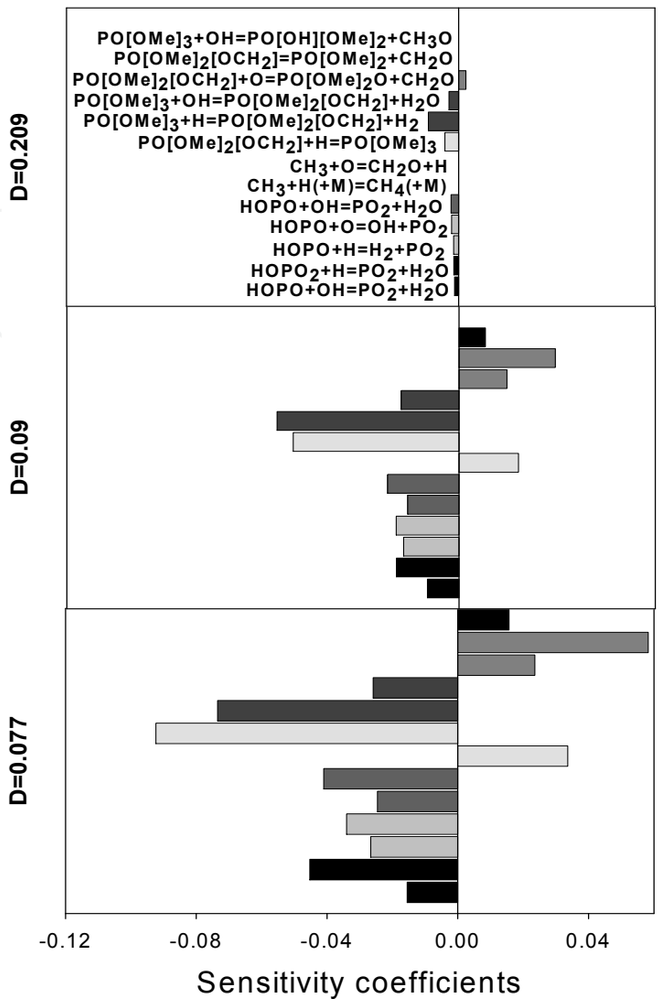

Fig. 10. Sensitivity coefficients of speed of $H_2/O_2/N_2$ flame (ϕ = 1.6, D = 0.077, 0.09, 0.209) doped with 0.04% TMP to rate constants of 13 key reactions of the inhibition mechanism (Jayaweera et al., 2005) involving P-containing species.

3.3 The mechanism for inhibition of hydrocarbon flames at atmospheric pressure

The inhibition effectiveness of hydrocarbon flames by phosphorus-containing inhibitors also increases with the rise of fuel excess in unburnt gases.

The burning velocities of propane–air and methane–air flames were measured on a flat burner using the heat flux method (De Goey et al., 1993; Van Maaren et al.,1994). This technique allows burning velocities to be measured with much higher accuracy (3% for stoichiometric flames and 5–10% for lean and rich flames) over a wide range of equivalence ratios.

Experimental data (Rybitskaya et al., 2007) on the burning velocities of propane–air and methane–air flames without additives (Fig. 11.) are in good agreement with literature data obtained using the same method (Bosschaart et al., 2004).

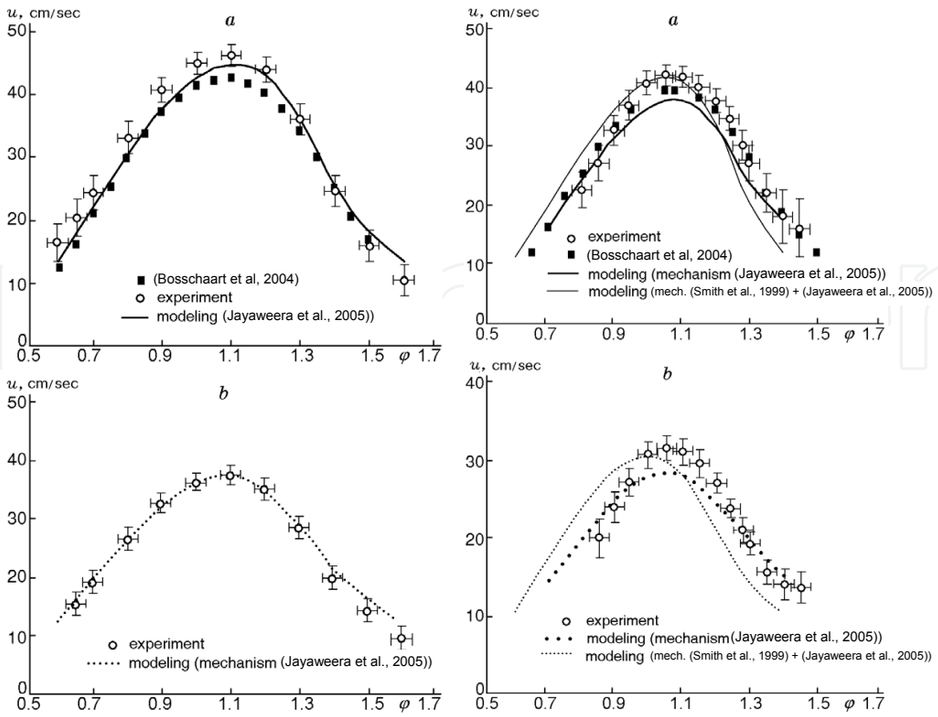

Fig. 11. Burning velocity of a propane–air flame (left) and methane-air flame (right) versus equivalence ratio without (a) and with the addition of 600 ppm TMP (b).

A comparison of the experimental data and modeling results for flames without additives and with 0.06% TMP showed to be in a satisfactory agreement for propane flames and differ somewhat for methane–air flames (Rybitskaya et al., 2007). For methane–air flames, the predictions using the GRI 3.0 mechanism are in better agreement with the experimental data for near stoichiometric flames, whereas the mechanism (Jayaweera, et al., 2005) provides a better agreement for lean and rich flames. Figure 12 presents the inhibition effectiveness of propane–air and methane–air flames by TMP, which is defined as $F = (u_0 - u)/u_0$, where u_0 and u are the burning velocities of the undoped and doped flames, respectively. The simulation predicts that the effectiveness increases with φ up to 1.3 and 1.2 for C_3H_8 and CH_4 flames, respectively, and then decreases in the region of rich flames. In the experiments, the inhibition effectiveness is also observed to decrease sharply in rich flames, whereas in lean and near-stoichiometric flames, the experimental dependence $F(\phi)$ is weakly expressed. The discrepancies between the simulation and measurement data may be due to drawbacks of both the mechanism for the reactions involving OPCs and the hydrocarbon combustion mechanisms. This is supported by the fact that two different kinetic schemes of hydrocarbon combustion (Jayaweera, et al., 2005; Smith et al., 1999) used in burning velocity calculations for TMP-doped flames with the same set of TMP reactions yield somewhat differing results. It noteworthy that the hydrocarbon combustion mechanisms used in the calculations have previously been tested by various researchers by comparing simulation and experimental results flame speed, structure, ignition delay in shock waves, and oxidation in a flow reactor. Therefore, the application of the two different hydrocarbon combustion mechanisms (Jayaweera, et al., 2005; Smith et al., 1999) allows estimating how these models influence the predicted speed of TMP-doped flames.

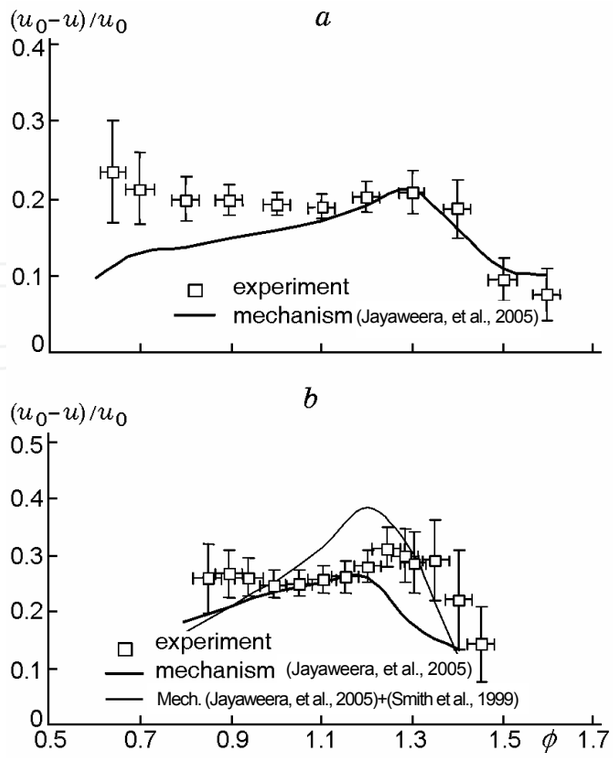

Fig. 12. Inhibition effectiveness versus equivalence ratio in propane–air (a) and methane–air (b) flames with the addition of TMP.

As the modeling results depend on a mechanism for hydrocarbon combustion, it is reasonable to performed modeling using several kinetic schemes. As can be seen from Fig. 11b, although these two different models give differing absolute values of F for $\phi \approx 1.2$, the resulting dependences $F(\phi)$ are qualitatively similar. The burning velocity simulation for a hydrogen–air flame (at p = 1 bar and T_0 = 298 K) without additives and with 0.1% TMP predicts the inverse dependence of the inhibition effectiveness. Figure 13 shows flame velocity sensitivity coefficients versus ϕ for changes in the rate constants of the most important reactions in TMP-doped propane–air and hydrogen–air flames. The sensitivity coefficients were determined by the formula $[(u - u_{5A})/u] \times 100\%$, where u and u_{5A} are the burning velocity calculated using the mechanism [(Jayaweera, et al., 2005) and the flame speed calculated using the same mechanism modified the pre-exponential factor of the reaction rate constant increased by a factor of five. Thus, the reactions PO_2+ H+M = HOPO+M and $HOPO_2$+H = PO_2+H_2O are the most significant in lean propane–air flames because these flames are dominated by compounds of phosphorus with a greater degree of oxidation, such as PO_2 and $HOPO_2$. The same reaction $HOPO_2$+H = PO_2+H_2O makes a significant contribution to the inhibition of lean hydrogen–air flames. For rich propane–air flames, the major contribution to the inhibition comes from the reaction HOPO + OH = PO_2 + H_2O, which is responsible for the sharp decrease in the effectiveness at ϕ = 1.3. The sensitivity coefficient dependence of this reaction (see Fig. 13a) correlates with the dependence of the inhibition effectiveness of TMP (see Fig. 12a): both have a maximum at $\phi \approx 1.3$.

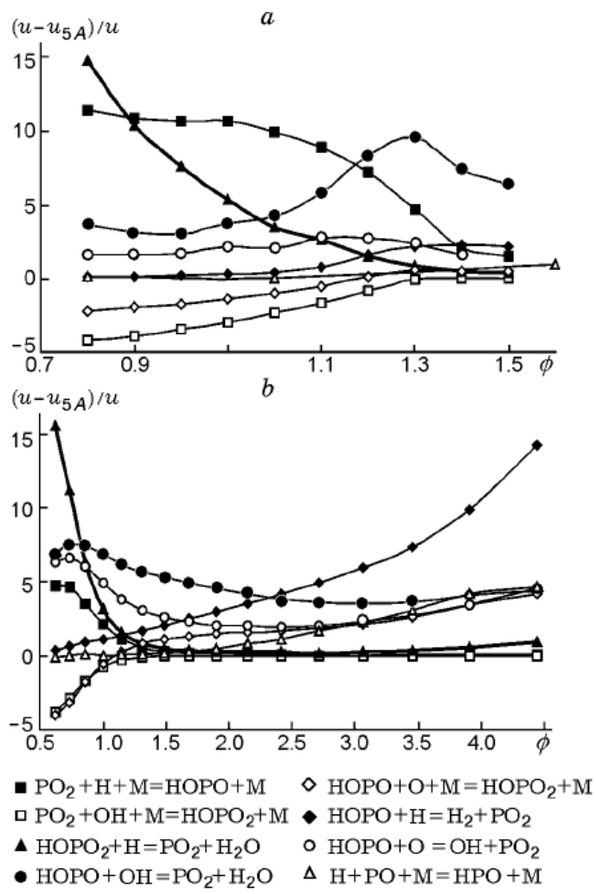

Fig. 13. Burning velocity sensitivity coefficients versus reaction rate constants in propane–air (a) and hydrogen–air (b) flames doped with TMP.

For rich hydrogen–air flames at $\phi > 2.5$, the highest contribution to the inhibition comes form the reaction HOPO+H = H_2 + PO_2, which, together with the other reactions, is responsible for an increase in the inhibition effectiveness as ϕ rise. Thus, the differences in the behavior of the inhibition effect of hydrocarbon–air and hydrogen– air flames occurs due to changes in the importance of the reactions of radicals with the phosphorus-containing products of TMP combustion. The curves of the inhibition effectiveness versus φ correlate with the those of the concentrations of H atoms and OH radicals versus in the chemical reaction zone ϕ of TMP- doped flames. Figure 14 presents the maximum concentrations of H and OH radicals in propane–air flames without additives and doped with TMP and their relative decrease versus equivalence ratio. As can be seen from the figure, the curve of the relative decrease in the radical concentration ($\Delta C_i/C_i$) and the curve of the inhibition effectiveness (see Fig. 12) have a break at $\phi = 1.3$, which indicates a direct relationship between the decrease in the concentration of the active radicals and the effect of the TMP additive. Similar curves for hydrogen–air flames are presented in Fig. 15. The reduction in the inhibition effectiveness in rich hydrocarbon flames may be due to an increase in the concentration of organophosphorus products of incomplete TMP destruction in the postflame zone at high equivalence ratios.

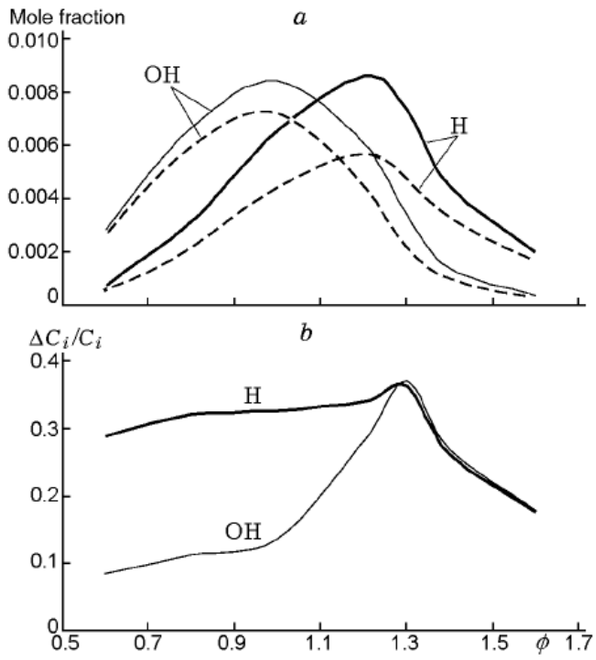

Fig. 14. Maximum concentrations of active radicals in propane–air flames (a) without additives (solid curves) and doped with 0.06% TMP (dashed curves) and the relative decrease in the concentrations (b).

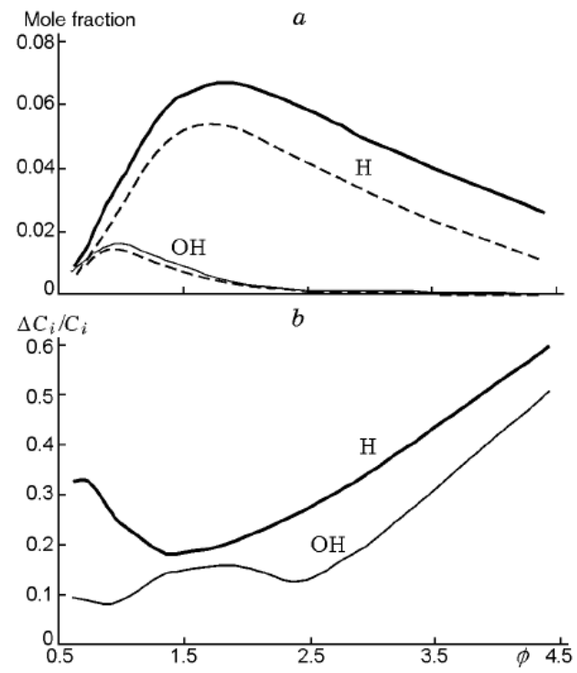

Fig. 15. Maximum concentrations of active radicals in hydrogen–air flames (a) without additives (solid curves) and with 0.1% TMP (dashed curves) and the relative decrease in the concentrations (b).

Species such as CH_3PO, CH_3PO_2, CH_3OPO, CH_3OPO_2, and CH_2OPO_2 are probably ineffective or incapable of catalyzing the recombination of H and OH radicals; therefore, a rise of their concentration in the combustion products leads to a decrease in the concentration of active species and inhibition effectiveness. Figure 16 demonstrates the ratio of the total concentration of CH_3PO, CH_3PO_2, CH_3OPO, CH_3OPO_2, and CH_2OPO_2 in the post-flame zone of propane–air and methane–air flames to the TMP loading versus equivalence ratio. These data obviously demonstrate that the sharp increase in the total concentration of organophosphorus products is observed in propane–air flames at $\phi = 1.4$, this almost coinciding with the maxima in the effectiveness curves in Fig. 12. It is noteworthy that, for the methane–air flames, the similar inhibition effectiveness curve has a maximum at $\phi = 1.2$–1.3 and a sharp increase in the total concentration of the organophosphorus products is observed at the same ϕ. Therefore, the accumulation of the catalytically ineffective organophosphorus intermediates in the rich OPCs-doped flame reduces the inhibition effectiveness.

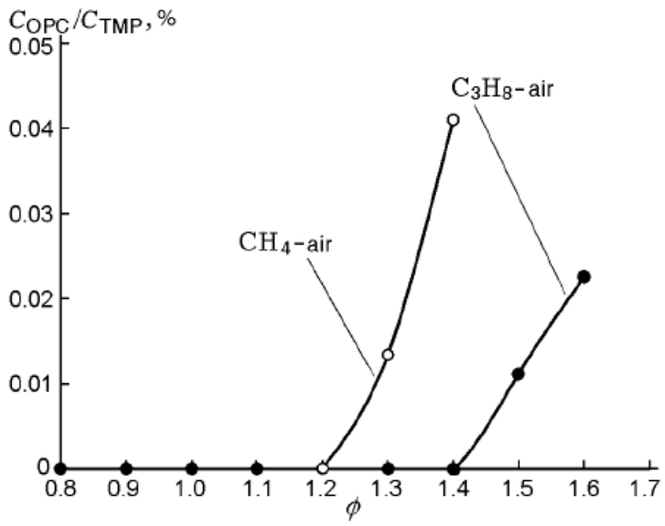

Fig. 16. Total concentration of CH_3PO, CH_3PO_2, CH_3OPO, CH_3OPO_2, and CH_2OPO_2 normalized to the initial TMP concentration in the flame (C_{OPC}/C_{TMP}) versus equivalence ratio.

One of the important combustion characteristics of premixed mixtures are flammability concentration limits (FCLs). The effect of various fire suppressants and inhibitors (chlorofluorohydrocarbons, bromine-containing hydrocarbons) on the FCLs of hydrocarbon–oxygen mixtures has been studied earlier (Saito et al., 1995; Shebeko et al., 2000) but the effect of OPCs have not been examined. Investigation of the inhibitors (including OPCs) influence on the FCLs allows, on the one hand, to evaluate the possibilities of their use as fire suppressants, and, on the other hand, to validate the inhibition mechanism by comparing experimental and modeling results. At present, there are a number of methods for determining FCLs, e.g. the method proposed by Coward and Jones (Coward & Jones, 1952); the standard method (State Standard No. 12.1.044-89; Baratov et al., 1990); a method using a cylindrical burner (Ishizuka, 1991; Hichens et al., 1999). In practice, these and other methods give different values for the FCLs of the same

combustible mixture, the results being greatly dependent on the design features of the experimental setups. In addition, there are a number of factors that are difficult to take into account in modeling but which have an appreciable influence on FCLs. The most important of them are the heat losses due to radiation and convection, the influence of the source and method of flame ignition, and the flame stretching effects (due to the presence of velocity gradients) (Ishizuka, 1991; Hertzberg, 1976). The opposed-flow burner method proposed by Law et al. (Law et al. 1986) to determine FCLs allows one to minimize the effect of heat losses on test results and to control the flame stretching. Law et al. (Law et al. 1986) used this method for determining FCLs of methane– and propane/air mixtures. It was also employed in (Womeldorf et al., 1995; Womeldorf & Grosshandler, 1996; Grosshandler et al., 1998) to determine the flammability limits of mixtures of fluorochlorohydrocarbons and air. Knyazkov et al (Knyazkov et al., 2008) used this method to study the effect of TMP additives on FCLs of methane–air mixtures. A significant advantage of the opposed-flow burner method for determining FCLs is that processes in this system can be modeled using detailed kinetic schemes. This allows one, by comparing calculated and experimental results, to obtain new data on the kinetic inhibition mechanism and to improve the employed kinetic scheme in order to increase the calculation accuracy.

The experimental setup used to determine FCLs of premixed combustible mixtures doped with OPCs is an opposed-flow burner equipped with a gas supply system and a system for supplying additives of the substances studied. TMP was added to both flows of the combustible mixture by two saturators. The required TMP vapor concentration was achieved by placing the saturators in a water bath at a thermostatically controlled temperature. It is known that the effect of any inhibitor on a flame is due to thermal-physics and chemical factors.

Experimental curves of the extinction velocity gradient K_{ext} for methane–air flames with and without TMP additives (in the TMP concentration range of 0–0.5% by volume) versus volumetric concentration of methane in the mixture are given in Fig. 17. For comparison, the figure also gives data for methane–air mixtures doped with CF_3Br. The obtained experimental points K_{ext} (values at various concentrations of CH_4 and a specified concentration of TMP) are approximated by lines which extrapolate the data to the value of $K_{ext} = 0$. Figure 17 gives data for the methane concentrations near the lower (Fig. 17a) and upper (Fig. 17b) flammability limits of the gas mixture studied. The methane concentrations in the mixture corresponding to the upper or lower flammability limits of the combustible mixture with and without additives were determined by the points of intersection of the straight lines with the abscissa. The data presented in Fig. 17 were used to obtain dependences of the upper and lower FCLs of methane– air mixtures on the volumetric concentrations of TMP and CF_3Br.

These dependences are given in Fig. 18; for comparison, the figure also shows the data for the concentration limits of CH_4/air/CF_3Br mixtures at a temperature of ≈353 K obtained by Saito et al. (Saito et al., 1995) using a cylindrical burner. As can be seen from Fig. 18, the flammability limits of CH_4/air mixtures are 4±0.2% CH_4 (the lower limit) and 16.2 ± 0.2% CH_4 (the upper limit).

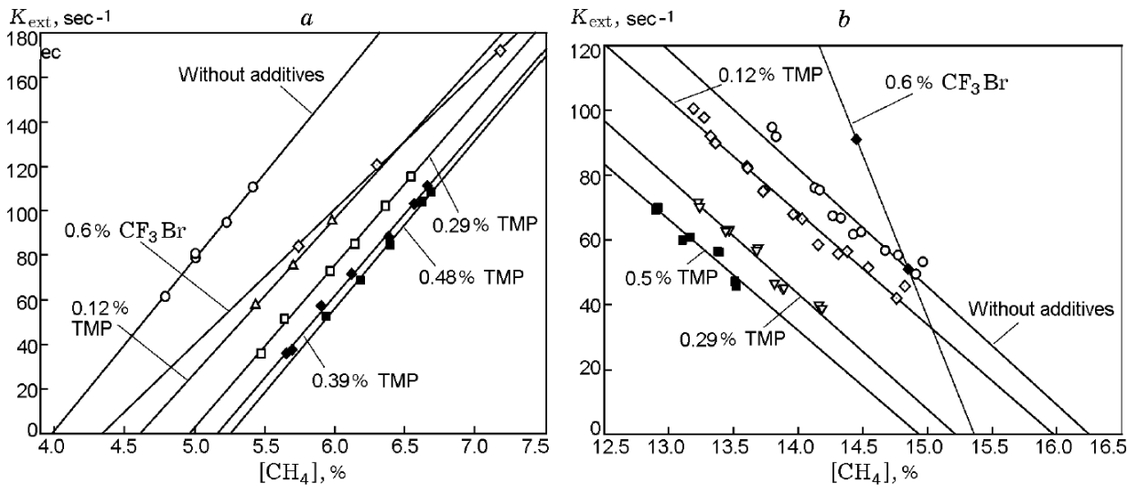

Fig. 17. Dependence of the extinction velocity gradient on methane concentration extrapolated to the value of K_{ext} = 0 for various TMP contents in the mixture: (a) lean flame; (b) rich flame.

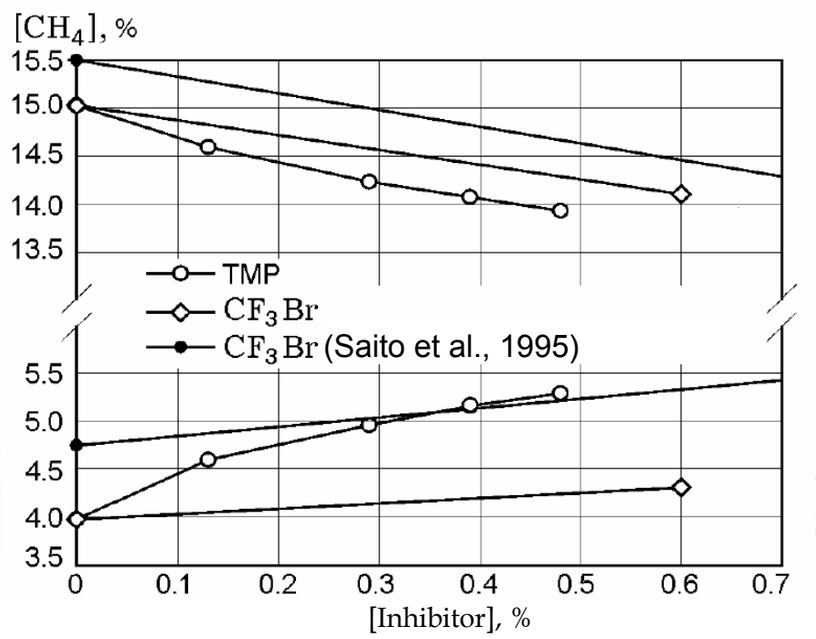

Fig. 18. Upper and lower flammability concentration limits of methane–air mixtures versus volumetric concentration of the inhibitor (CF_3Br and TMP).

These data differ from the results of Saito et al. (Saito et al., 1995), according to which the flammability limits are in the methane concentration range of 4.75–15.5%. The observed difference is obviously not due to the difference between the temperatures of the initial combustible mixtures in the experiments because it is only ≈15 K, but it is due, as noted above, by the difference between the techniques used in the studies. It should also be noted

that if the experiments described in the present paper were performed at a temperature of the initial mixture of ≈298 K, the flammability concentration limits would be somewhat narrower. Hichens et al. showed (Hichens et al., 1999) that changing the temperature of the initial methane–air mixture by 70 K led to an approximately 0.5% change in each limit. In view of this, the concentration limit for these conditions should be 4.5–15.7 % CH_4. An analysis of the literature (Saito et al., 1995; Baratov et al., 1990; Ishizuka, 1991; Hichens et al., 1999; Womeldorf & Grosshandler, 1996), shows that, for methane– air mixtures under normal conditions, various methods give lean flammability limits in the [CH_4] range of 4.0 to 5.3% and rich limits in the range of 13.8–15.6%. Thus, the values of the lower and upper limits obtained in the work fall in these ranges, i.e., the employed technique yields reasonable results in agreement with literature data. Experiments on determining the effect of CF_3Br additives on the flammability limits made it possible, on the one hand, to reproduce the data of (Saito et al., 1995) and thus to test the procedure of determining the limits, and, on the other hand, to compare the effects of TMP and CF_3Br on the FCLs. The experiments were performed at a 0.6% concentration of CF_3Br in the combustible mixture. Because the flammability limits of the combustible mixture without additives do not coincide with those obtained in (Saito et al., 1995), we compare data on changes in the limit (upper or lower) at specified concentrations of CF_3Br. From Fig. 18 it is evident that, according to (Saito et al., 1995), the addition of 0.6% CF_3Br leads to a 1% decrease in the upper concentration limit for methane and a ≈0.5% increase in the lower limit. This agrees with the result obtained in our work using an opposed-flow burner. The addition of TMP to the combustible mixture, as is seen from Fig. 18, narrows the flammability concentration limits. The relative effect of TMP reduces as its concentration is increased; in particular, the addition of 0.12% TMP changes both limits for [CH_4] by ≈0.5%, and to change the limits by 1%, it is necessary to add ≈0.4% TMP. It is worth noting that, in contrast to CF_3Br, the addition of TMP has the same effect on both the lower and the upper concentration limit within the experimental error. For example, the addition of 0.48% TMP reduces the upper limit for [CH_4] by ≈1.1% and increases the lower limit by ≈1.3%. As noted above, the effect of CF_3Br on the upper limit is twice that on the lower limit. The addition of 0.3% TMP increases the lower limit four times more effectively than the addition of CF_3Br of the same concentration. Furthermore, the addition of TMP reduces the upper limit two times more effectively than the addition of CF_3Br. It is known that many flame inhibitors, such as fluorinated hydrocarbons (for example, CF_3Br), influence the upper and lower concentration limits differently: they reduce the upper limit more strongly and increase the lower limit less strongly (Saito et al., 1995; Shebeko et al., 2000). This effect is due mainly to the fact that the addition of an inhibitor to a combustible mixture leads to a change in the equivalence ratio, and, thus, to a reduction in both concentration limits for methane, and, as result, to different effectiveness of the additive for the upper and lower limits. In the experiments with the addition of TMP to the combustible mixture, this effect was not observed. Figure 19 gives experimental and calculated dependences $K_{ext} = f([CH_4])$ for flames without additives and doped with 0.12% TMP. It is evident that, in both cases, the experimental dependences $K_{ext} = f([CH_4])$ agree better with the predicted dependences for lean mixtures than for rich mixtures. Figure 20 gives experimental and calculated dependences of the upper and lower flammability concentration limits on the volumetric concentration of TMP in methane–air mixtures. It is evident that, for both the

doped undoped flames, the predicted lean concentration limits are also in better agreement with the corresponding experimental values than the values of the rich limits. In particular, the value of 4.2% predicted for the of the flame without TMP is in good agreement with the experimental result of 4%. According to the modeling data, the increase in the lower concentration limit due to the addition of 0.12% TMP to the combustible mixture was 0.7%, which also agrees with the experimental data (within the measurement error). The predicted rich concentration limit for the undoped flame is seen to fit well to the experimental value. However, there is a difference between the experimental data and modeling results for the reduction in the rich limit due to the addition of 0.12% TMP to the mixture. This is most likely due to the drawbacks of the kinetic mechanism. For example, the mechanism does not take into account heavy hydrocarbons which are known to form in rich flames. The experimental finding that TMP has the same effect on both the lower and upper concentration limits (in contrast to, for example, CF_3Br, which, as noted above, changes the upper limit more strongly than the lower limit) agrees qualitatively with data (Korobeinichev et al., 2007) on the effect of the addition of TMP on the velocity of premixed propane–air flames with various equivalence ratios. It was found that the inhibition effectiveness determined from the decrease in the flame propagation velocity drops with increasing ϕ in the range of $\phi > 1.3$ (see explanation above).

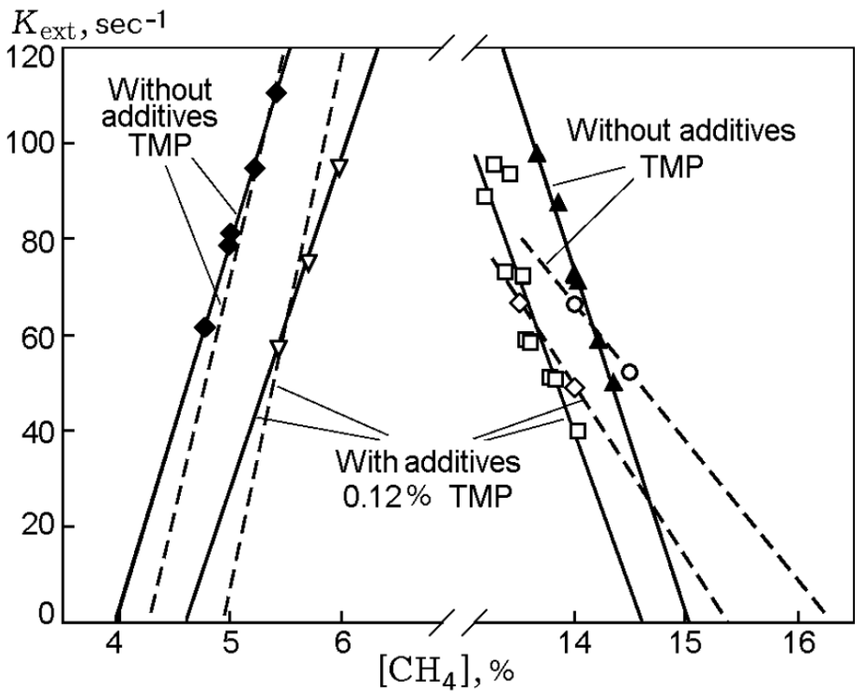

Fig. 19. Experimental and calculated extinction velocity gradients versus volumetric concentration of CH_4 in methane–air mixtures (without additives and doped with 0.12% TMP): the solid curves are extrapolations of the experimental data, and the dashed curves are extrapolations of the calculation data.

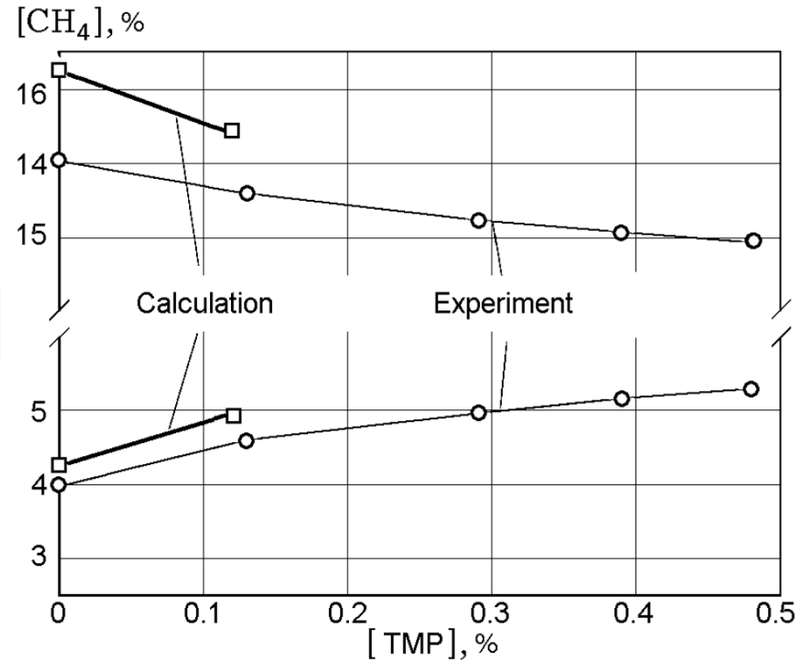

Fig. 20. Experimental and calculated upper and lower flammability concentration limits of methane–air mixtures versus volumetric concentration of TMP.

4. Iron-containing compounds

4.1 The mechanism for inhibiting hydrogen flames at atmospheric pressure

The first studies of iron-containing species (ICS) as flame inhibitors were performed in the early 1960s. Lask and Wagner (Lask & Wagner, 1962) were the first to measure the effect of iron pentacarbonyl $Fe(CO)_5$ on the speed of H_2/air flame and to show that it was 2 orders of magnitude greater than that of CF_3Br. Miller et al. (Miller et al., 1963) studied the effect of certain inhibitors, including $Fe(CO)_5$, on the speed of H_2/air flames for various stoichiometry and the inhibitor concentration of 0.5% by volume. Unfortunately, addition of $Fe(CO)_5$ at this concentration greatly changed the fuel equivalence ratio of the initial flame because 2.5% by volume of carbon monoxide was formed in the flame and as a result the effect of iron alone was difficult to assess.

An increased interest in metal-containing compounds, including iron pentacarbonyl and ferrocene $Fe(C_6H_6)_2$ as flame inhibitors, has arisen after the ban on the production of halogenated fire-extinguishing agents (such as CF_3Br) with a high ozone depletion potential. Searches for new inhibitors and fire suppressants have led scientists to pay attention to ICS compounds. Reinelt and Linteris (Reinelt & Linteris, 1996) studied the effect of $Fe(CO)_5$ and ferrocene on premixed laminar flame speeds and extinction strain rates of opposed-jet diffusion flames. The inhibition effectiveness was shown to strongly depend upon the dopant loading; the maximum inhibition was achieved at a concentration as low as 100 μL/L (μL/L is equivalent to parts per million by volume) and was then little affected by a further increase in the concentration. Rumminger et al. (Rumminger et al., 1999) attribute this to the formation of iron-containing particles in the flame, resulting in a reduction in the

gas-phase concentration of iron species (which are responsible for flame inhibition). According to data (Reinelt & Linteris, 1996), an increase in the oxygen volume fraction in a O_2/N_2 mixture reduces the inhibition effect. This may be due to the combustibility of iron pentacarbonyl and ferrocene.

Linteris et al. (Linteris et al., 2000a) performed experimental and modeling studies of the effect of $Fe(CO)_5$ and $Fe(C_6H_6)_2$ additives on the speed of a $CH_4/O_2/N_2$ flame. The numerical study was based on a kinetic model (Rumminger et al., 1999), which provided a good fit to experimental results. Ferrocene, whose molecule contains more fuel than that of iron pentacarbonyl, showed a lower inhibition effect than $Fe(CO)_5$.

Rumminger et al. (Rumminger et al., 1999) determined the key chemical processes responsible for flame inhibition

$$FeOH+H = FeO+H_2$$

$$FeO+H_2O = Fe(OH)_2$$

$$Fe(OH)_2+H=FeOH+H_2O$$

This is equivalent to the recombination of hydrogen atoms $H + H=H_2$. The catalytic recombination of O atoms also involves three elementary reactions

$$Fe+O_2 + M = FeO_2 + M$$

$$FeO_2 +O = FeO + O_2$$

$$FeO + O = Fe + O_2$$

The role of the formation of iron-containing particles in the inhibition of hydrogen and methane flames by a $Fe(CO)_5$ additive was studied by Rumminger & Linteris (Rumminger & Linteris, 2000a, 2002). The results showed that the formation of iron particles reduced the inhibition effect of the iron pentacarbonyl additive. This supports the hypothesis of a gas-phase mechanism for flame inhibition by ICS.

Experimental studies of cup-burner flame suppression by metallic compounds (Linteris et al., 2004) have provided further evidence for the gas-phase mechanism of inhibition by ICS. Models ignoring solid-phase formation in flame predict the greater inhibition effect than experimental data.

Spatial variations in the temperature and concentration of atomic iron in a low-pressure lean (φ = 0.37) $H_2/O_2/Ar/Fe(CO)_5$ flame were measured using laser-induced fluorescence (Wlokas et al., 2009; Staude et al., 2009a). Iron pentacarbonyl was found to decompose in the flame to produce atomic iron, which was then transformed to iron oxides and hydroxides. On the basis of a previously developed mechanism (Rumminger et al., 1999), a reduced 12-step mechanism for flame inhibition by $Fe(CO)_5$ was developed and validated by comparing measured and simulated concentration profiles of atomic iron.

A low-pressure, rich (φ=2.3), laminar, premixed propene/oxygen/argon flame doped with ferrocene was studied experimentally using molecular beam mass spectrometry (MBMS) and laser-induced fluorescence (LIF) and by numerical simulations (Tian et al., 2009). The

flame temperature was obtained by two-line OH LIF measurements, and the additive was found to increase the postflame temperature by 40 K. MBMS analysis of the species profiles of important intermediates in flames with and without ferrocene doping showed a slight increase in the maximum concentration of species, such as CH_2O, C_5H_5, and C_6H_6. At the same time, the dopant slightly decreased the maximum concentration of the propargyl radical C_3H_3, which is known to be an intermediate in the formation of soot precursors. The MBMS measurements showed that the flame velocity decreased with the addition of ferrocene, which was not predicted by the model.

Staude and Atakan (Staude & Atakan, 2009b) carried out equilibrium calculations for iron-doped hydrogen/oxygen/argon and propene/oxygen/argon gas mixtures under combustion-relevant conditions. It is noteworthy that condensed Fe-containing compounds were considered in the calculations. The focus was on iron intermediates and the conditions under which condensed phases of iron or iron species could be expected in the flame. The stoichiometry (ϕ= 0.37, 1, and 2.3), temperature (1000-2500 K), and pressure (0.03-1 bar) were varied, allowing for a prediction of which gas-phase iron species might be expected in measurable concentrations under the flame conditions used. The effect of the sampling probe on the composition of the combustion products, which are cooled during probing, was discussed.

The developed model for flame inhibition by iron compounds was continually validated by comparing the measured and modeled burning velocity of near-stoichiometric flames doped with $Fe(CO)_5$ and ferrocene. A significant progress in understanding the features of the inhibition chemistry under lean and rich conditions was made by measuring and simulating the H_2/air flame speed over a wide range of equivalence ratios (Fig. 21) (Gerasimov et al., 2011). Furthermore, Gerasimov et al. (Gerasimov et al., 2011) performed unique measurements of the spatial variation of concentration of some of $Fe(CO)_5$ destruction products (Fe, FeO_2, FeOH, and $Fe(OH)_2$) in premixed atmospheric-pressure $H_2/O_2/N_2$ flame using probing molecular beam mass spectrometry with soft ionization by electron impact. A comparison between experimental and numerical results revealed that the mechanism used in the study (Rumminger et al., 1999) satisfactorily predicts speeds of atmospheric-pressure H_2/air flames over a wide range of equivalence ratios and concentration profiles FeO_2 and $Fe(OH)_2$ in the flame.

Shvartsberg et al. (Shvartsberg et al., 2010) showed that the inhibition effectiveness (expressed as the relative decrease of the flame speed as the dopant is added) substantially depends upon the equivalence ratio of unburnt gases: the minimum effectiveness is observed at $\phi \approx 2$, and the maximum effectiveness is observed in lean flames (Fig. 22.). At the same time the same authors demonstrated that the maximum total rate of the active species (H, O, and OH)) consumption is observed in stoichiometric flame that at first glance seems contrary to the effectiveness curves (Fig. 23). This illusory contradiction was adjusted by suggesting that the inhibition effectiveness over a wide range of equivalence ratios of hydrogen flames depends not only by the rate of chain termination in Fe-involving reactions but also by the rate of chain branching ($H + O_2 = O + OH$). This suggestion was supported by comparing curves of the inhibition effectiveness and the ratio of the integrated production rates of chain carriers (H + O + OH) to the chain-branching rate (Shvartsberg et al., 2010). The products of atomic iron oxidation in H_2/air flames mainly catalyze H atom recombination, and the recombination rate is largely determined by the concentration of

iron hydroxides FeOH and $Fe(OH)_2$. It happens because the rate of consumption of O atoms is much lower than that of H atoms and its sum with rate of OH production gives a value close to zero. OH radicals are produced in Fe-involving reaction in atmospheric-pressure H_2/air flame all over range of equivalence ratios (Shvartsberg et al., 2010).

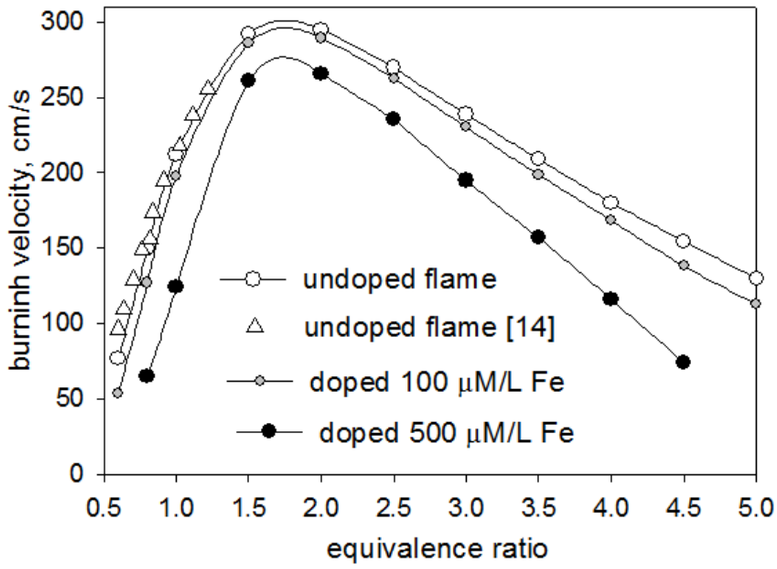

Fig. 21. Speed of H_2/air flames without additives and doped with 100 and 500 μL/L atomic iron versus the equivalence ratio at a pressure of 0.1 MPa. Lines, modeling results; symbols, literature data.

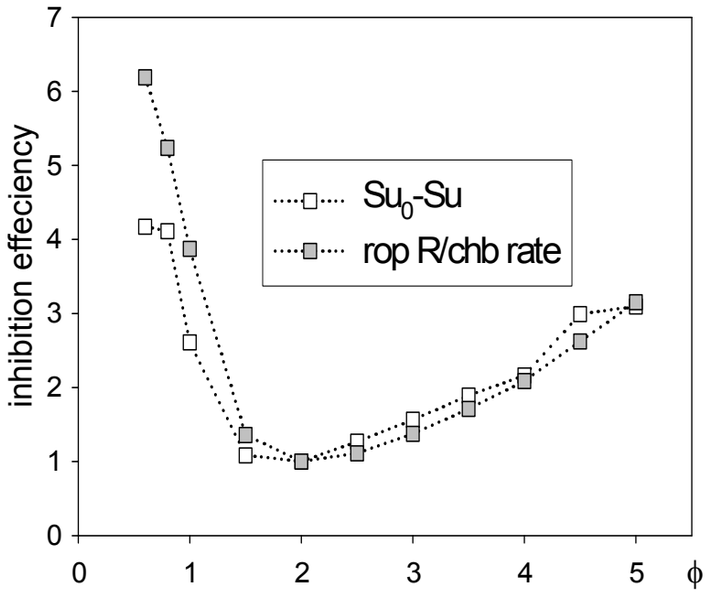

Fig. 22. Inhibition effectiveness of atmospheric-pressure H_2/air flames doped with 100 μL/L atomic iron, expressed as (1) the decrease in flame speed because of doping (open symbols) and (2) the ratio of the integrated production rates of chain carriers (H + O + OH) to the chain-branching rate (gray symbols).

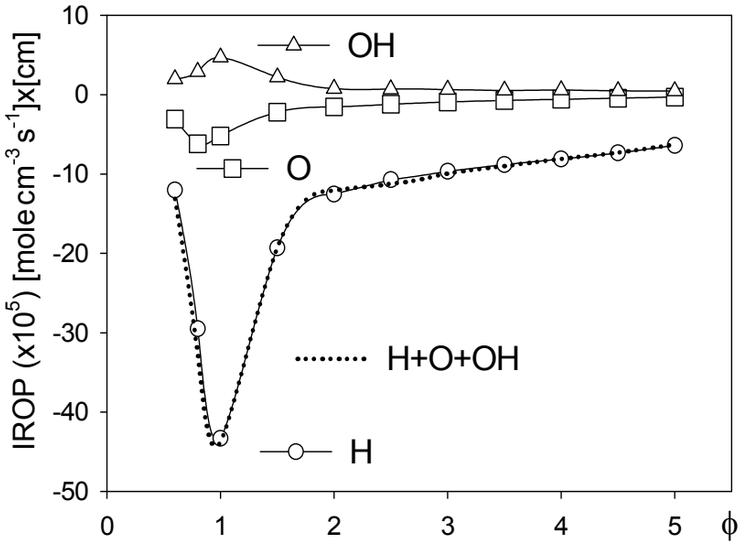

Fig. 23. Integrated production rate (mol cm^{-3} s^{-1})x(cm) of H, O, and OH and the total production rate of all of these species in reactions involving ICS in atmospheric-pressure H_2/air flames doped with 100 μL/L atomic iron versus the equivalence ratio.

According to (Shvartsberg et al., 2010) the variation of net rate of production/consumption of the chain carriers in the Fe-involving reactions versus ϕ is mainly associated with a variation of ICS composition and variation of concentration of the chain carriers in the reaction zone of the flames with flame stoichiometry. The change of the flame temperature with ϕ plays minor role in variation of the rate of production of the active flame species. It may be explained by relatively low activation energies of the Fe-involving reactions from the mechanism (Linteris et al., 2000a), which do not exceed 6500 J/mol.

The chemical processes responsible for changes in the production rates of H, O, and OH as ϕ changes were identified. Three flames were chosen for the analysis: a lean flame with ϕ=0.6, a stoichiometric flame with the maximum rate of radical production, and the richest flame with ϕ=5. The rate of H atom production in separate reactions was calculated, and the key reactions for each of the chosen flames were determined. In addition, to evaluate the role of each reaction qualitatively the authors (Shvartsberg et al., 2010) calculated the contribution of each reaction to the total rate of H consumption, considering only the reactions involving ICS. It was found out that, regardless of the flame equivalence ratio, the key reactions responsible for H atom removal are as follows:

$$FeOH+H = FeO+H_2$$

$$Fe(OH)_2+H = FeOH+H_2O$$

This was also shown previously for a stoichiometric $CH_4/O_2/N_2$ flame (Rumminger et al., 1999). In the richest flame (ϕ=5), the reaction $FeO_2 + H + M = FeOOH + M$ also makes a noticeable contribution to the removal of H atoms from the flame.

Using analogues approach, the key Fe-involving reactions of O atoms consumption were found (Shvartsberg et al., 2010):

$$FeOH + O = FeO + OH$$

$$FeO_2 + O = FeO + O_2$$

$$Fe + O_2 = FeO + O$$

Although reaction of FeOH with O atom is a key reaction of O atoms consumption, it is unlikely to contribute to the inhibition effectiveness because it transforms one chain carrier to another (O → OH). This fact largely determines the symmetry of the O and OH curves of rate of production of these species.

5. Super-effective inhibitors

Among the chemically active inhibitors (such as phosphorus-, bromine-, iodine- containing compounds, etc.), compounds of alkali metals are the least studied experimentally, which is explained by their very low volatility.

The minimum extinguishing concentrations (MECs) are one of the most important characteristics of flame suppressants, proving estimates of prospects for their future application. Shmakov et al. (Shmakov et al., 2006) applied the cup-burner technique to study a number of recently synthesized organophosphorus compounds and inorganic and organic potassium salts (K_3PO_4, $KOOCH_3$, KOOCCOOK, and $K_4[Fe(CN)_6]$). Aqueous solutions of the examined salts were fed through a nebulizer to the heated air flow in the same way as was done for OPCs. The mass median particle diameter of the salt solution aerosols was 10–20 μm, and after water evaporation, it decreased to 2–5 μm. The mass-median diameter of the aerosol particles was determined with the aid of a five stage impactor (Korobeinichev et al., 2003). Concentrations near the cup were found by sampling the air–aerosol flow through the aerosol filter and determining the mass of the aerosol deposited on it. The MECs of the examined compounds were calculated taking into account the effect of water contained in the solution. Most of the experiments were performed at a constant temperature of the air flow of 75°C. Under these conditions, the aerosol particles of the liquid substances completely vaporized.

Among the OPCs tested, the most effective flame suppressant (in terms of the volume concentration of vapor) is $[(CF_3)_2CHO]_2P(O)CF_3$; it is followed (in decreasing order of the MEC) by $[(CF_3)_2CHO]_2P(O)C_2H_5$; $[(CF_3)_2CHO]_3P$; $(CF_3CH_2O)_2P(O)CF_3$; $(CF_3CH_2O)_3P$; $[(CF_3)_2CHO]_2P(O)CH_3$. The minimum extinguishing concentration of such effective fire suppressant as $(CF_3CH_2O)_3P$ varies from 1 to 3% (by volume). The results of experiments (Table 2) on extinguishing a diffusion *n*-heptane/air flame by aqueous salt solutions show that potassium salts are an order of magnitude more effective than OPCs and halons (Linteris, 2001).

Salt	minimal extinguishing concentration	
	mole fraction (×100)	g/m^3
K_3PO_4	No extinguishing at 1%	
$KOOCH_3$	0.25	10.9
KOOCCOOK	0.13	9.6
$K_4[Fe(CN)_6]$	0.035	6.6

Table 2. The studied salts and their minimal extinguishing concentration

The effectiveness of flame suppression by an organic salt per a molecule is directly proportional to the number of potassium atoms in it. The possible mechanism for flame inhibition by potassium salts is following:

$$\text{Potassium salt} \rightarrow K_2O, KOH, \text{etc.}$$

$$KOH + H \rightarrow K + H_2O$$

$$K + OH + M \rightarrow KOH + M$$

$$\text{Total: } H + OH \rightarrow H_2O$$

A distinction is observed for $K_4[Fe(CN)_6]$ because this salt contains not only potassium but also iron. Some iron compounds, for example, $Fe(CO)_5$, are known to be effective flame inhibitors. In the case of $K_4[Fe(CN)_6]$, potassium and iron act jointly in extinguishing flames but the obtained data do not provide a quantitative estimate of the synergetic effect of their joint action.

The expected effectiveness of K_3PO_4 should be much higher than the effectiveness of the OPC but the experiments disprove this assumption. In flame, thermally stable potassium phosphate K_3PO_4 does not dissociate into reactive inhibitors – potassium oxides and phosphorus oxyacids. Thus, the use of combined flame suppressants based on OPCs and MCCs is not promising.

The obtained data suggest very intense chemical reactions of inhibition in the flames doped with alkali metal compounds. The inhibition chemistry of the alkali metals has been studied insufficiently and may become an object of future research.

6. Conclusion

Summarizing the obtained data on inhibition chemistry, we came to following conclusions.

1. The effectiveness of a certain inhibitor depends on features of its combustion chemistry, flame stoichiometry and conditions (pressure). These developments should be necessarily taken into consideration in the case of practical application of an inhibitor.
2. In fact, it is not valid to expect an effective flame inhibitor to be also effective for auto-ignition. Moreover, the same compound can promote the auto-ignition. As an example we can mention iron pentacarbonyl that inhibits atmospheric-pressure H_2/air flames but can reduce the ignition delay of the same mixtures.
3. The inhibition effectiveness of flames with appreciably different equivalence ratio is explained by not only different rate of the chain carriers consumption. A flame with maximum burning velocity (or near-stoichiometric flame) all other things being equal, are inhibited less effectively than rich or lean flames.
4. The inhibition chemistry of essentially rich hydrocarbon flames with equivalence ratio close to the flammability limit is not adequately investigated. It is explained by very complex combustion chemistry of soot and its precursors formation, which interaction with inhibitor was not explored.
5. A search for novel alternative chemically active inhibitors should be continued and it must be based on fundamental understanding of combustion chemistry of certain

compounds. Simultaneously the search should involve various flames over a wide range of equivalence ratios, auto-ignition of various mixtures, and other objects of study.

7. References

Baratov, A.; Korol'chenko, A. & Kravchuk, G. (1990). *Fire and Explosion Hazard of Substances and Materials and Means of Fire Suppression: Handbook,* Khimiya, Moscow [in Russian]

Biordi, J.; Lazarra, C. & Papp, J. (1974). Molecular beam mass spectrometry applied to determining the kinetics of reactions in flames. I. Empirical characterization of flame perturbation by molecular beam sampling probes. *Combustion and Flame,* Vol.23, No. 1, pp. 73-82, ISSN 0010-2180

Bolshova, T. & Korobeinichev, O. (2006). Promotion and Inhibition of a Hydrogen–Oxygen Flame by the Addition of Trimethyl Phosphate, *Combustion, Explosion, and Shock Waves*, Vol. 42, No. 5, pp. 493–502, ISSN 0010-5082

Bonne, U.; Jost, W. & Wagner, H. (1962). Iron Pentacarbonyl in CH_4-O_2 and Air Flames, *Fire Res. Abstr. Rev.,* Vol. 4, pp. 6–18

Bosschaart, K.;de Goey, L. & Burgers, J. (2004). The laminar burning velocity of flames propagation in mixtures of hydrocarbons and air measured with the heat flux method, *Combustion and Flame,* Vol. 136, No. 3, pp. 261–269, ISSN 0010-2180

Burton, K.; Ladouceur, H. & Fleming J. (1992). An Improved Noncatalytic Coating for Thermocouples. *Combust. Sci. Technol.,* Vol. 81, pp. 141-145, ISSN 0010-2202

Coward, H. & Jones, G. (1952). Limits of flammability of gases and vapors, *Bureau of Mines Bull. No. 503,* Washington, D.C., USA

Curran, H.; Gallagher, S.; Conaire, M. & Simmie J. (2003). Comprehensive Modelling Study of Methane Oxidation. *Proceedings of 3rd European Combustion Meeting*, Orleans, France, October 2003

Curran, H.; Jayaweera, T.; Pitz, W. & Westbrook, C. (2004). A Detailed Modeling Study of Propane Oxidation, *Proceedings of Western States Section meeting of The Combustion Institute,* Davis, CA, USA, March 2004

De Goey, L.; Van Maaren, A. & Quax, R. (1993). Stabilization of Adiabatic Premixed Laminar Flames on a Flat Flame Burner. *Combust. Sci. Technol.,* Vol. 92, p.201-207, ISSN 0010-2202

Dodonov, S.; Karpov, A. & Pevzner, A. (1990) Information-measuring system for research of streams are charged particles. USSR Inventor's Certificate No. 1457716, *Byull. Izobret.*, No. 47. p.272

Egolfopoulos, F. & Law. C. (1990).An experimental and computational study of the burning rates of ultra-lean to moderately-rich $H_2/O_2/N_2$ laminar flames with pressure variations, *Proc. Combust. Inst.,* Vol. 23, pp. 333-340, ISSN 1540-7489

Gerasimov, I.; Knyazkov, D.;Shmakov, A.; Paletsky, A.; Shvartsberg, V.; Bolshova, T. &Korobeinichev, O. (2011).Inhibition of Hydrogen-Oxygen Flames by Iron Pentacarbonyl at Atmospheric Pressure, *Proc. Combust. Inst.,* Vol. 33, No.2, pp. 2523-2529, ISSN 1540-7489

Glaude, P.; Curran H.; Pitz, J. &Westbrook, C. (2000). Kinetic Study of the Combustion of Organophosphorus Compounds, *Proc. Combust. Inst.*, Vol. 28, pp. 1749-1756, ISSN 1540-7489

Grosshandler, W.; Donnelly, M. & Womeldorf, C. (1998). Lean flammability limit as a fundamental refrigerant property: Phase III, *NIST Interim Tech. Report,* September 2011, Available from: http://www.fire.nist.gov/bfrlpubs/fire98/PDF/f98061.pdf

Hastie, J. & Bonnell, D. (1980).Molecular Chemistry of Inhibited Combustion Systems, *National Bureau of Standards,* Washington, D.C., 1980, NBSIR 80–2169

Hertzberg, M. (1976). The theory of flammability limits: natural convection, *Bureau of Mines.* Rep. of Investigation No. RI-8127

Hichens, R.; Dlugogorski, B. & Kennedy, E. (1999). Advantages and drawbacks of tubular flow burner for testing flammability limits,*Proceedings of Halon Options Technical Working Conference HOTWC-1999,* Albuquerque, NM, USA, April 1999.

Hughes, K.; Turanyi, T. & Pilling, M. (2001). The Leeds methane oxidation mechanism, ver 1.5, In: *Combustion Simulation,* September 2011, Available from: http://garfield.chem.elte.hu/Combustion/methane.htm

Ishizuka, S. (1991). Determination of flammability limits using a tubular flame geometry, *J. Loss Prev. Process. Ind.*, Vol. 4, pp. 185–193, ISSN 0950-4230

Jayaweera, T.; Melius, C.; Pitz, W.; Westbrook, C.; Korobeinichev, O.; Shvartsberg, V.; Shmakov, A.; Rybitskaya, I. & Curran, H. (2005). Flame Inhibition by Phosphorus-Containing Compounds over a Range of Equivalence Ratios, *Combustion and Flame,* Vol. 140, No.1-2 pp. 103-115, ISSN 0010-2180

Kaskan, W. (1957). The Dependence of Flame Temperature on Mass Burning Velocity. *Proc. Combust. Inst.*, Vol. 6, pp. 134-143, ISSN 1540-7489

Kee, R.; Crcar, J.; Smooke, M. & Miller J. (1989a). A Fortran Program for Modeling Steady Laminar One-Dimensional Premixed Flames, *Sandia National Laboratories,* 1989, Report No. SAND85–8240

Kee, R.; Rupley, F. & Miller, J. (1989b). CHEMKIN-II:A Fortran Chemical Kinetics Package for the Analysis of the Gas Phase Chemical Kinetics, *Sandia National Laboratories,* 1989, Report No. SAND89–8009B

Knyazkov, D.; Shmakov, A. & Korobeinichev, O. (2007). Application of molecular beam mass spectrometry in studying the structure of a diffusive counterflow flame of CH_4/N_2 and O_2/N_2 doped with trimethylphosphate, *Combustion and Flame,* Vol. 151, No.1-2 pp. 37-45, ISSN 0010-2180

Knyazkov, D.; Yakimov, S. Korobeinichev, O. & Shmakov, A. (2008). Effect of Trimethylphosphate Additives on the Flammability Concentration Limits of Premixed Methane–Air Mixtures,*Combustion, Explosion, and Shock Waves,* Vol. 44, No. 1, pp. 9–17, ISSN 0010-5082

Korobeinichev, O.; Chernov, A. & Shvartsberg, V. (1994). Mass-spectrometric Investigation of the Structure of a Stoichiometric $H_2/O_2/Ar$ Flame Doped with Trimethylphosphate and N-Tributylphosphate, P*reprint of Paper - American Chemical Society, Division of Fuel Chemistry,* Vol. 39, No. 1, pp. 139-197, Washington, D.C., USA

Korobeinichev, O.; Ilyin, S.; Mokrushin, V. & Shmakov, A. (1996). Destruction Chemistry of Dimethyl Methylphosphonate in $H_2/O_2/Ar$ Flame Studied by Molecular Beam Mass Spectrometry. *Combust. Sci. Technol.,* Vol. 116–117, pp. 51-67, ISSN 0010-2202

Korobeinichev, O.; Shvartsberg, V.; Il'in, S.; Chernov, A. & Bolshova, T. (1999a). Laminar Flame Structure in a Low-Pressure Premixed $H_2/O_2/Ar$ Mixture. *Combustion, Explosion, and Shock Waves*, Vol. 35, No. 3, pp.239-244, ISSN 0010-5082

Korobeinichev, O.; Shvartsberg, V. & Chernov, A. (1999b). The Destruction Chemistry of Organophosphorus Compounds in Flames—II: Structure of a Hydrogen–Oxygen Flame Doped with Trimethyl Phosphate. *Combustion and Flame,* Vol. 118, pp.727-732, ISSN 0010-2180

Korobeinichev, O.; Bolshova, T.; Shvartsberg, V.; Chernov, A. & Mokrushin, V. (1999c). Inhibition Effect of TMP on $CH_4/O_2/Ar$ and $H_2/O_2/Ar$ Flames, *Proceedings of Halon Options Technical Working Conference HOTWC-1999,* Albuquerque, NM, USA, April 1999.

Korobeinichev, O.;Ilyin, S.; Shvartsberg, V. & Chernov, A. (1999d). The Destruction Chemistry of Organophosphorus Compounds in Flames—I: Quantitative Determination of Final Phosphorus-Containing Species in Hydrogen-Oxygen Flames, *Combustion and Flame,* Vol. 118, pp. 718-726, ISSN 0010-2180

Korobeinichev, O.; Ilyin, S.; Bolshova, T.; Shvartsberg V. & Chernov A. (2000). The Chemistry of the Destruction of Organophosphorus Compounds in Flames—III: The Destruction of DMMP and TMP in a Flame of Hydrogen and Oxygen. *Combustion and Flame,* Vol. 121, pp. 593-609, ISSN 0010-2180

Korobeinichev, O.; Bolshova, T.; Shvartsberg V. & Chernov A. (2001). Inhibition and Promotion of Combustion by Organophosphorus Compounds Added to Flames of CH_4 or H_2 in O_2 and Ar, *Combustion and Flame*, Vol. 125, pp. 744-751, ISSN 0010-2180

Korobeinichev, O.; Shmakov, A.; Shvartsberg, V.; Knyazkov, D.; Makarov, V.; Koutsenogii, K.; Samsonov, Yu.; Nifantev, E.; Kudryavtsev I.; Goryunov, E.; Nikolin, V. & Kaledin,V. (2003). Study of Effect of Aerosol and Vapors of Organophosphorus Fire Suppressants on Diffusion Heptane and Premixed C_3H_8/Air Flames, *Proceedings of Halon Options Technical Working Conference HOTWC-2003,* Albuquerque, NM, USA, May 2003.

Korobeinichev, O.; Shvartsberg, V.; Shmakov, A.; Bolshova, T.; Jayaweera, T.; Melius, C.; Pitz, W.; Westbrook, C. & Curran, H. (2005). Flame Inhibition by Phosphorus-Containing Compounds in Lean and Rich Propane Flames, *Proc. Combust. Inst.*, Vol. 30, pp. 2353-2360, ISSN 1540-7489

Korobeinichev, O.; Shvartsberg, V.;Shmakov, A.; Knyazkov, D. & Rybitskaya, I. (2007). Inhibition of Atmospheric Lean and Rich $CH_4/O_2/Ar$ Flames by Phosphorus-Containing Compound, *Proc. Combust. Inst.*, Vol. 31, pp. 2741-2748, ISSN 1540-7489

Korobeinichev, O.; Rybitskaya, I.; Shmakov, A.; Chernov, A.; Bolshova, T. & Shvartsberg, V.(2009). Inhibition of atmospheric-pressure $H_2/O_2/N_2$ flames by trimethylphosphate over range of equivalence ratio, *Proc. Combust. Inst.,* Vol. 32, pp. 2591-2597, ISSN 1540-7489

Lask, G. &Wagner, H. (1962). Influence of additives on the velocity of laminar flames, *Proc. Combust. Inst.,* Vol. 8, pp. 432-438, ISSN 1540-7489

Law, C.; Zhu, D. & Yu, G. (1986). Propagation and extinction of stretched premixed flames, *Proc. Combust. Inst.,* Vol. 21, pp. 1419–1426, ISSN 1540-7489

Li, J.; Zhao, Zh.; Kazakov, A. & Dryer, F. (2004). An Updated Model and Discussion of Modeling Challenges in High-Pressure H_2/O_2 Flames, *Int. J. Chem. Kinetics,* Vol.36, No. 10, pp. 566-575, ISSN 1097-4601

Linteris, G.; Rumminger, M.; Babushok ,V. & Tsang, W. (2000a). Flame inhibition by ferrocene and blends of inert and catalytic agents, *Proc. Combust. Inst.,* Vol. 28, pp. 2965-2972, ISSN 1540-7489

Linteris, G. (2001). Suppression of cup-burner diffusion flames by supereffective chemical inhibitors and inert compounds, *Proceedings of Halon Options Technical Working Conference HOTWC-2001,* Albuquerque, NM, USA, April 2001.

Linteris, G.; Katta, V. & Takahashi, F. (2004). Experimental and numerical evaluation of metallic compounds for suppressing cup-burner flames, *Combustion and Flame,* Vol. 138, pp. 78-96, ISSN 0010-2180

MacDonald, M.; Gouldin, F. &Fisher, E. (2001). Temperature dependence of phosphorus-based flame inhibition, *Combustion and Flame,* Vol. 124, No. 4, pp. 668-683, ISSN 0010-2180

Mackie, J.; Bacskay, G.; & Haworth, N. (2002). Reactions of Phosphorus-Containing Species of Importance in the Catalytic Recombination of H + OH: Quantum Chemical and Kinetic Studies, *J. Phys. Chem. A,* Vol. 106, No. 45, pp. 10825-10830, ISSN 1089-5639

Miller, D.; Evers, R. & Skinner, G. (1963). Effects of various inhibitors on hydrogen-air flame speeds, *Combustion and Flame,* Vol. 7, pp. 137-142, ISSN 0010-2180

Reinelt, D. & Linteris, G. (1996). Experimental study of the inhibition of premixed and diffusion flames by iron pentacarbonyl, *Proc. Combust. Inst.,* Vol. 26, pp. 1421-1428, ISSN 1540-7489

Rumminger, M.; Reinelt, D.; Babushok, V. & Linteris, G. (1999). Numerical study of the inhibition of premixed and diffusion flames by iron pentacarbonyl, *Combustion and Flame,* Vol. 116, pp. 207-219, ISSN 0010-2180

Rumminger, M. & Linteris, G. (2000). The role of particles in the inhibition of premixed flames by iron pentacarbonyl, *Combustion and Flame,* Vol. 123, pp. 82-94, ISSN 0010-2180

Rumminger, M. & Linteris, G. (2002). The role of particles in the inhibition of counterflow diffusion flames by iron pentacarbonyl, *Combustion and Flame,* Vol. 128, pp. 145-164, ISSN 0010-2180

Rybitskaya, I.; Shmakov, A. & Korobeinichev, O. (2007). Propagation Velocity of Hydrocarbon–Air Flames Containing Organophosphorus Compounds at Atmospheric Pressure, *Combustion, Explosion, and Shock Waves,* Vol. 43, No. 3, pp. 253–257, ISSN 0010-5082

Saito, N.; Saso, Y.; Liao, C.; Ogawa, Y. & Jnoue, Y. (1995). Flammability peak concentrations of halon replacements and their function as fire suppressant, *Halon Replacements: Technology and Science, ACS Symp. Ser., Amer. Chem. Soc.*, pp. 243–257

Shebeko, Yu.; Azatyan, V.; Bolodian, I.; Navzenya, V.; Kopylov, S. Shebeko, D. & Zamishevski, E. (2000). The influence of fluorinated hydrocarbons on the combustion of gaseous mixtures in a closed vessel, *Combustion and Flame,* Vol. 121,pp. 542–547, ISSN 0010-2180

Shmakov, A.; Korobeinichev, O.; Shvartsberg, V.; Knyazkov, D.; Bolshova, T. & Rybitskaya, I. (2004). Inhibition of Premixed and Non-Premixed Flames with Phosphorus-Containing Compounds, *Proc. Combust. Inst.,* Vol. 30, No. 2, pp. 2342–2352, ISSN 1540-7489

Shmakov, A.; Korobeinichev, O.; Shvartsberg, V.; Yakimov, S.; Knyazkov, D.; Komarov, V. & Sakovich, G. (2006). Testing ogranophosphorus, organofluorine, and metal-containing compounds and solid-propellant gas-generating compositions doped with phosphorus-containing additives as effective fire suppressants, *Combust. Explos. Shock Waves,* Vol. 42, No. 6, pp.678–687, ISSN 0010-5082

Shvartsberg, V.; Bolshova, T. &Korobeinichev O.(2010). Numerical Study of Inhibition of Hydrogen/Air Flames by Atomic Iron, *Energy and Fuels,* Vol.24, No. 3, pp 1552–1558, ISSN 0887-0624

Smith, G.; Golden, D.; Frenklach, M.; Moriarty, N.; Eiteneer, B.; Goldenberg, M.; Bowman, T.; Hanson, R.; Song, S.; Gardiner, W.; Lissianski, V. & and Qin, Z. (1999).GRIMec3.0, In: *GRI-Mech Home Page*, September 2011, Available from: http://www.me.berkeley.edu/gri_mech/

Staude, S. & Atakan, B. (2009). An Investigation of Equilibrium Iron Thermochemistry in Flames,*The Open Thermodynamics Journal*, Vol. 3, pp. 42-46, ISSN 1874-396X

Staude, S.; Hecht, C.; Wlokas, I.; Schulz, C.; Atakan, B. (2009). Experimental and Numerical Investigation of $Fe(CO)_5$ Addition to a Laminar Premixed Hydrogen/Oxygen/Argon Flame, *Z. Phys. Chem.*, Vol. 223, pp. 639-649, ISSN 0942-9352

Tian, K.; Li, Z.; Staude, S.; Li, B.; Sun, Z.; Lantz, A.; Alden, M. & Atakan B. (2009). Influence of ferrocene addition to a laminar premixed propene flame: Laser diagnostics, mass spectrometry and numerical simulations, *Proc. Combust. Inst.,* Vol. 32, pp. 445–452, ISSN 1540-7489

Twarowski, A. (1993a). The influence of phosphorus oxides and acids on the rate of H + OH recombination. *Combustion and Flame,* Vol. 94, pp. 91-107; ISSN 0010-2180

Twarowski, A. (1993b). Photometric determination of the rate of H2O formation from H and OH in the presence of phosphine combustion products, *Combustion and Flame,* Vol. 94, pp. 341-348, ISSN 0010-2180

Twarowski, A. (1995). Reduction of a phosphorus oxide and acid reaction set, *Combustion and Flame*, Vol. 102, pp. 41-54, ISSN 0010-2180

Twarowski, A. (1996). The Temperature Dependence of H+OH Recombination in Phosphorus Oxide Containing Combustion Gases, *Combustion and Flame,* Vol. 105, pp. 407-413, ISSN 0010-2180

Van Maaren, A.; Thung, D. & De Goey, L. (1994). Measurement of Flame Temperature and Adiabatic Burning Velocity of Methane/Air Mixtures. *Combust. Sci. Technol.*, Vol. 96, pp. 327-344, ISSN 0010-2202

Werner, J. & Cool, T. (1999). Kinetic Model for the Decomposition of DMMP in a Hydrogen/Oxygen Flame. *Combustion and Flame,* Vol. 117, pp. 78-98, ISSN 0010-2180

Wlokas, I.; Staude, S.; Hecht, C.; Atakan, B. & Schulz, C. (2009). Measurement and simulation of Fe-atom concentration in premixed $Fe(CO)_5$-doped low-pressure H_2/O_2 flames, *Proceedings of the European Combustion Meeting ECM-2009,* Vienna, Austria, April 2009.

Womeldorf, C.; King, M.; & Grosshandler, W. (1995). Lean flammability limit as a fundamental refrigerant property: Phase I, In: *NIST Interim Tech. Report,* September 2011,Available from: http://www.fire.nist.gov/bfrlpubs/fire95/PDF/f95083.pdf

Womeldorf, C. & Grosshandler, W. (1996). Lean flammability limit as a fundamental refrigerant property: Phase II, *NIST Interim Tech. Report,* September 2011, Available from: http://www.fire.nist.gov/bfrlpubs/fire96/PDF/f96072.pdf

Zachariah, M. & Smith, O. (1987). Experimental and numerical studies of sulfur chemistry in $H_2/O_2/SO_2$ flames, *Combustion and Flame,* Vol. 69, No. 2, pp. 125-139, ISSN 0010-2180

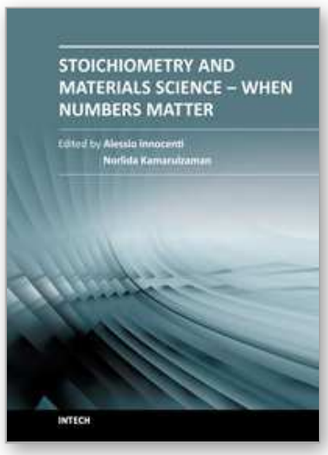

Stoichiometry and Materials Science - When Numbers Matter

Edited by Dr. Alessio Innocenti

ISBN 978-953-51-0512-1
Hard cover, 436 pages
Publisher InTech
Published online 11, April, 2012
Published in print edition April, 2012

The aim of this book is to provide an overview on the importance of stoichiometry in the materials science field. It presents a collection of selected research articles and reviews providing up-to-date information related to stoichiometry at various levels. Being materials science an interdisciplinary area, the book has been divided in multiple sections, each for a specific field of applications. The first two sections introduce the role of stoichiometry in nanotechnology and defect chemistry, providing examples of state-of-the-art technologies. Section three and four are focused on intermetallic compounds and metal oxides. Section five describes the importance of stoichiometry in electrochemical applications. In section six new strategies for solid phase synthesis are reported, while a cross sectional approach to the influence of stoichiometry in energy production is the topic of the last section. Though specifically addressed to readers with a background in physical science, I believe this book will be of interest to researchers working in materials science, engineering and technology.

InTech Europe
University Campus STeP Ri
Slavka Krautzeka 83/A
51000 Rijeka, Croatia
Phone: +385 (51) 770 447
Fax: +385 (51) 686 166
www.intechopen.com

InTech China
Unit 405, Office Block, Hotel Equatorial Shanghai
No.65, Yan An Road (West), Shanghai, 200040, China
中国上海市延安西路65号上海国际贵都大饭店办公楼405单元
Phone: +86-21-62489820
Fax: +86-21-62489821

IntechOpen